Zienkiewicz, O. C. (1977), The *Finite Element Method*, McGraw-Hill, New York.
Zienkiewicz, O. C., and Shiomi, T. (1984), Dynamic behavior of saturated porous media; the generalized Biot formulation and its numerical solution, *Int. J. Num. Anal. Meth. Geomech.*, **8**, 71–96.
Zienkiewicz, O. C., Watson, M., and King, I. P. (1968), A numerical method of viscoelastic creep analysis, *Int. J. Mech. Sci.*, **10**, 807–27.

Mathematical Modeling of Creep and Shrinkage of Concrete
Edited by Z. Bažant

Chapter 5

Probabilistic Models[†]

5.1 INTRODUCTION

In designing concrete structures, it has become a common practice to consider the probabilistic aspects of various factors involved, for example, the compressive strength of concrete (Mirza *et al.*, 1979), similarly the probabilistic design of general structures (e.g. Shinozoka and Shao, 1973; Ang and Tang, 1975; Anderson *et al.*, 1978; Turkstra and Madsen, 1980; Turkstra and Reed, 1981; Lind *et al.*, 1985). This tendency is reflected in a certain design code (e.g. CEB–FIP, 1978). For a designer, in order to ensure the safety of a concrete structure, the variation of the factors involved in the problem, as well as the mean value, is a prime concern. To predict the deformation of a concrete structure due to creep, it is important to know not only the mean value of the ultimate creep, but the extreme values that have a certain specified small probability of being exceeded. Up until now, most of the research works have been concerned with trying to predict creep and shrinkage using deterministic models that best fit the test data available in the literature. For various types of deterministic models for creep and shrinkage, see, for example, Hansen (1960), Bažant and Wu (1974), Bažant and Osman (1976), Bažant and Panula (1978, 1980). Comparison of these models are also reported by Bažant and Panula (1978, 1980), and Bažant and Chern (1982). A deterministic model has its merit as far as predicting the average behaviour for 'best estimates' of the input variables, but an estimate of the expected statistical variation is lacking. Its quantitative estimate can be obtained only by probabilistic or statistical means. Current deterministic formulations of models of concrete creep also seem to have reached a limit of refinement beyond which further attempts of development may be of little value if the randomness of the creep phenomenon is neglected. Instead of trying to develop more sophisticated deterministic creep models, it seems worth while to formulate stochastic models for concrete creep and thus in a direct way take into account the uncertainties in the description of the phenomenon, whatever source these uncertainties may have.

References on statistical treatment of creep of concrete were rather limited up

[†] Principal author: T. Tsubaki. Prepared by RILEM TC69 Subcommittee 5, the members of which were Z. P. Bažant, O. Buyukozturk, C. Huet, H. O. Madsen, T. Tsubaki (Chairman), and F. H. Wittmann.

to several years ago (Cinlar *et al.*, 1977). Most of the work has treated creep in connection with long-time deflections of reinforced concrete beams (Manuel and MacGregor, 1967; Tadros *et al.*, 1974; Bridge, 1979). Certain statistical models have been suggested for deflection (ACI Committee 435, 1972; Nasser and Marzouk, 1981). However, the deflection problem is not equivalent to the problem of constitutive behaviour of the material. Many factors are involved in the deflection problem and it is difficult to separate them. This is due to the fact that the data analysed pertain to beams tested in flexure without control of humidity conditions. As far as the prediction of long-time creep from short-time tests under controlled conditions is concerned, Brooks and Neville (1975) and Brooks (1984) introduced statistical distribution of certain material parameters into an assumed deterministic law and looked for correlation between long-time and short-time creep, using a regression analysis. They suggested a linear form for the relationship between long-time and short-time creep and they imposed both the mean value and variance on the model. Kesler *et al.* (1965) also reported on this subject. Properly, however, extrapolation of creep data obtained under controlled conditions should be treated by means of a stochastic process. One of the early works that dealt with creep as a stochastic process is the paper by Benjamin *et al.* (1965). Consideration of some more general models is also suggested in some other works (Cornell, 1964; Gabrielson, 1966). Recently, however, a number of different approaches to deal with creep in probabilistic or statistical manners have been reported (e.g. Çinlar *et al.*, 1977; Çinlar and Bažant, 1979; Ditlevsen 1982b; Bažant and Zebich, 1983; Bažant and Chern, 1984), which will be introduced in the subsequent sections. Statistically tractable creep data were also scarce in the literature and even those available do not follow a consistent statistical procedure, especially as far as measuring times are concerned. This makes it different to verify the choice of any stochastic model in a strict statistical sense. On the other hand, in recent years, more light has been thrown on the physical mechanism of creep itself (Bažant, 1974; Wittman, 1982), which may be used as basis for the choice of the stochastic model.

Checking the deflections of actual concrete structures caused by creep and shrinkage of concrete, significant statistical variation is observed. For information on long-time observation of creep data and the field measurements, see, for example, the works by Jávor (1982) and Russell *et al.* (1982). The variation of creep and shrinkage phenomenon is caused by various factors. As the external factors, the change of environmental conditions, such as temperature and humidity, may be considered. The effect of these factors are, in general, predominant over other factors. The internal factors, on the other hand, are the variation of the quality and the mix composition of the materials used in concrete and the variation due to the internal mechanism of creep and shrinkage. The statistical variation may be attributed to the following uncertain factors.

Internal uncertain factors

1. Variation due to the stochastic nature of the physical mechanism of creep and shrinkage *per se*.
2. Variation due to material properties. (In general, the coefficient of variation of material properties such as compressive strength and elastic modulus is approximately 10 per cent or less.)

External uncertain factors

3. Variation due to environmental conditions. (Creep and shrinkage are significantly influenced by the seasonal or daily change of weather, i.e. temperature and humidity.)
4. Variation due to external loads. (The structure is subjected to highly variable loads such as snow and live loads.)
5. Variation due to measuring technique.

Uncertain factors due to formula or modeling

6. Variation due to the choice of the formulas for predicting creep and shrinkage.
7. Variation due to the choice of the analytical methods such as simple quasi-elastic analysis and sophisticated finite element analysis.

Factor (1) is due to the randomness of the concrete microstructure and the creep or shrinkage increments. Unlike other sources of variation, the variation due to factor (1) may remain as the principal factor of uncertainty, since it is inherent in concrete itself and cannot be eliminated. Factor (2) can be eliminated only under well-controlled conditions such as those in a laboratory. In actual construction sites, it would be very difficult to eliminate the variation in the mix composition and the material quality. By factor (3), the drying condition of the concrete is affected and the amount of creep and shrinkage and the stresses caused by shrinkage are considerably influenced. Also, the material properties of concrete are affected by the environmental changes. Factor (4) may make the stress state higher or lower than the design stress level, yielding more or less creep strain than that expected. Also, the variation of the stress level may cause variation of the material properties. Factors (3) and (4), however, may be taken into account in the design a priori if the statistical parameters of the variations of loads and environmental conditions are known. As for factor (5), it is only in the measured data, and not in concrete itself. Therefore, this variation should not be included in a model for predicting creep or shrinkage. When field observations are made to update the probabilistic model and thus decrease the variation in the prediction of the further development of creep effects, then this variation must be explicitly included in the model

updating. By well-controlled experiments, the measuring error may be eliminated. The elimination of factor (6) may be the ultimate goal for the researchers in the field of creep and shrinkage of concrete. The formulas for creep and shrinkage used in a design code must be such that the prediction may be obtained with a minimum error. As for factor (7), it appears important to know the amount of errors caused by choosing a particular method of analysis. Needless to say, the method of analysis should be a reasonable one without complexity and over-simplification.

As described above, the statistical variation of creep and shrinkage of concrete is caused by both internal and external factors. Considering this fact, this chapter is divided into three parts. In the first part, the statistical variation of creep and shrinkage of concrete attributed to the internal mechanism of creep and shrinkage is considered. In Section 5.2, the difference between deterministic and probabilistic (stochastic) models is explained and a brief description on the micromechanism of creep and shrinkage is given. In Section 5.3, probabilistic models of creep making use of a Poisson process, a Markov process, a gamma process, and a white noise process are introduced. In the second part, other influencing factors on the statistical variation of creep and shrinkage, such as the effects of the material mix and composition, the environmental condition of the specimen, and the measuring technique are considered. In Section 5.4, a brief survey of experimental works is given and several statistical approaches for creep prediction are introduced. In the third part, i.e. in Sections 5.5 and 5.6, methods of analysis of concrete structures are introduced both for the internal and external influencing factors on creep and shrinkage. In relation to the above description, general information of the development in creep and shrinkage of concrete in both the deterministic the and probabilistic sense may be obtained from Neville (1970), ACI Committee (1971, 1972), Bažant (1974), Neville (1981), ACI Committee (1982), Bažant (1982a), Bažant and Panula (1982), Çinlar (1982), Huet (1982b), Task Committee (1982), American Concrete Institute (1983), Bažant (1983).

5.2 DETERMINISTIC AND PROBABILISTIC MODELS

In Sections 5.2 and 5.3, the probabilistic nature of the internal physical mechanism of creep and shrinkage, i.e. factor (1) in the previous section, will be considered.

5.2.1 Definitions

The definitions of deterministic and probabilistic (stochastic) models are stated as follows (Cornell, 1964).

There exist two basic approaches to the construction of a suitable mathematical model which describes the creep and shrinkage of concrete: the deterministic approach and the probabilistic (stochastic) approach. The deterministic approach, after the determination of a relation between the variables, leads to a prediction that, given certain values of these variables, a particular state or value of the process will be observed. On the other hand, the probabilistic model, which specifies the complete joint probability distribution of individual factors at each point of time, predicts the likelihood with which each of the possible states will be observed.

5.2.2 Stochastic nature of creep and shrinkage

Some conclusions on the stochastic properties of creep and shrinkage of concrete can be derived by considering their microscopic mechanisms. Based on the present state of knowledge, the mechanism of basic creep can be described as follows (Çinlar *et al.*, 1977).

Concrete is made up of aggregate and sand embedded in a matrix of hardened cement paste. The main solid component of this matrix is the cement gel between the sheet-like structures. The hardened cement paste matrix contains interconnected pores of different sizes. The largest pores, called macropores, are of round shape, contain capillary water, and are interconnected by a system of thinner pores. The thinnest ones, called micropores or gel pores, represent the gaps between the sheets. They are essentially laminar and some of them possibly tubular in shape, and they are only one to several molecules in thickness. The micropores contain water strongly held by solid surfaces, which could be regarded as hindered water or interlayer water. The micropores also contain relatively weakly held and partially mobile particles of solids bridging the gap between the opposite surfaces of the pores. The water in laminar micropores can exert on the pore walls a significant transverse pressure, called disjoining pressure. When a compressive load is applied on concrete, most of the resulting compression across the laminar micropores is carried by the solid particles bridging the pores. Water in the micropores receives only a small portion of the applied load because it has undoubtedly much smaller stiffness than the solid particles. The stress across the micropores causes certain solid particles to migrate slowly out of the compressed pores (Bažant, 1974) in the direction normal to the compressive stress (i.e. along the pores). The solid particles that can possibly migrate under load are held by bonds of various strengths and are subjected to various stresses. Those that are held weakly or receive higher stress are most likely to lose their bond (i.e. jump over their activation energy barrier) and migrate to a stress-free location or one of lower stress. As the number of weakly held and highly stressed particles becomes exhausted, the rate of migrations diminishes, causing a decline of the creep rate. As the particles leave the micropores, the transverse pressure (disjoining pressure) is relaxed and the applied load is transferred partly on to the elastic aggregate, partly on to other micropores. This also causes a decline of the creep rate. In addition, simultaneous

hydration, which fills available pores by additional cement paste opposing the deformation, causing further deceleration of creep. The presence of water in the micropores is essential for the migration to be possible. Thus, without water in the pores, as in predried concrete, there is almost no creep. At constant water content of concrete, movements of water along the pores are rather limited and play no significant role in creep. This is the case of basic creep. When water content varies, e.g. because of external drying, a large amount of water diffuses along the micropores. The movement of water endows the solid particles with greater mobility (Bažant, 1974) and causes an acceleration of the migration of solid particles along the micropores, thereby accelerating creep. This explains the phenomenon of drying creep. When the applied stress is purely volumetric, it causes the solid particles to migrate along the micropores into the largest, round-shaped pores (macropores) whose walls do not receive any pressure as a result of applied load. When the applied stress is purely deviatoric (shear), it causes the particles to migrate from the laminar micropores normal to the direction of the principal compressive stress into the laminar micropores normal to the direction of the principal tensile stress, and the passage of the particles does not have to intersect any of the macropores. For a general state of applied stress, including the case of uniaxial stress, both types of migration happen simultaneously. In addition, the random migration of particles would be significantly influenced by the random stress field caused by the local inhomogeneity which is inherent in a composite material such as concrete. This migration of solid particles and movement of gel water which takes place randomly in time and space may be considered as a stochastic process. Some stochastic creep models using this kind of micromechanism consideration are introduced in the subsequent section.

The mechanism of shrinkage of concrete may be decomposed into three parts (Wittmann, 1982), i.e. capillary shrinkage, chemical shrinkage, and drying shrinkage. Some shrinkage mechanisms classified as chemical shrinkage may take place without connection with the external drying condition. However, most of the dominant shrinkage mechanisms are related to the drying condition at the surface of a specimen. Therefore, the distribution of shrinkage strain is not uniform and depends on the geometry of the specimen or structure. This may make the statistical variation of shrinkage and also drying creep larger than that of basic creep. Due to the above fact, shrinkage is not a constitutive property in a strict sense. To model shrinkage as a part of a constitutive relation, it is necessary to consider the average deformation due to shrinkage. Therefore, unlike the mechanism of basic creep, it seems difficult to construct a stochastic process model for shrinkage. Çinlar (1982) may provide useful information on this subject. However, statistical models to predict the statistical parameters such as the mean and variance for shrinkage of concrete have been developed by some researchers. For these studies, see Bažant *et al.* (1985a, b).

5.2.3 Remarks

For other detailed description and classification of the mechanisms of creep and shrinkage, see Chapter 1 as well as the work of Wittmann (1982). On the cement paste microstructure, see the work of Young (1982). See, also Slate and Meyers (1971), Bažant (1972b, 1977, 1979).

5.3 PROBABILISTIC CONSTITUTIVE MODELS OF CREEP

As stated in the previous section, the creep and shrinkage of concrete are highly uncertain phenomena, the statistical variation of which is larger than that of strength and elastic modulus. The deformations of apparently identical concrete members under identical environmental conditions and subjected to identical stress history show deviations up to 20 or 30 per cent of the average values (Cinlar, 1982). The consequences of a large error in predicting creep and shrinkage may shorten the service life of concrete structures by, for example, loss of water tightness and corrosion of steel bars. Sometimes it may even lead to catastrophic collapse, as in creep buckling (e.g. Manuel and MacGregor, 1967; Bažant and Tsubaki, 1980b) or in the case of detrimental effects of creep and shrinkage on other types of structural failure. So far, in the prediction of the creep of concrete, the possibility of an inherent source of uncertainty in the microscopic creep process is either not taken into account or considered of no importance for the macroscopic phenomenon. In this section, therefore, some mathematical creep models are introduced to account for the internal sources of uncertainty of creep. To eliminate other sources of variation, only basic creep is considered. It will be shown that that such a probabilistic (stochastic) model enables statements to be made concerning the variation of the creep strain about its mean value; it yields not only the mean value but also the statistical parameters such as the variance and auto-covariance functions.

5.3.1 Poisson process and Markov process models

In the following, stochastic creep models using a Poisson process and a Markov process are introduced. A Poisson process is equivalent to a Markov process with independent increments. The works by Cornell (1964), Gabrielsen (1966), Benjamin *et al.* (1965), and Chow and Shah (1971) are introduced. The characteristic Markov restriction can be stated as 'given the present state of the process, the future is independent of how this state has been reached'. As for the Poisson process, it can be said that this process has no memory.

Following Hansen's deterministic model for basic creep (Hansen, 1960), creep strain is decomposed into three parts in Cornell's model (Cornell, 1964), i.e. creep strains due to viscous flow, delayed elasticity, and hydration. The viscous-flow portion of the basic creep of concrete under sustained compression has been

ascribed to the gradual squeezing of the viscous liquid portion of the paste from between the boundaries of crystalline particles of the cement paste. If the creep strain due to viscous flow is assumed proportional to the change in the amount of fluid remaining between these particles, and this volume is assumed to be made up of small discrete units, then, with the squeezing out of each unit, this population can be thought of as a process undergoing unit increases in size randomly in time. Therefore, a simple, non-homogeneous Markov birth process (non-homogeneous Poisson process) is chosen for this viscous-flow portion of basic creep. The birth-rate or transition intensity is a function of time, because of the time-dependent viscosity. The second part, i.e. the delayed-elastic portion of creep strain, is caused by the flow of water molecules (absorbed gel-water) out from within the skeleton of cement crystals and aggregate in the highly stressed areas of the concrete. With the departure of the molecules, the small amount of stress it carried is transferred to the surrounding elastic skeleton. The creep strain due to the delayed-elastic phenomenon may be proportional to the volume of water which moves from within the elastic skeleton to surrounding voids. However, the rate of the process is also proportional to the stress in the water to be squeezed out. This stress is decreasing as water is squeezed. Hence, the linear homogeneous Markov death process is chosen to model this process. The third part, i.e. the 'hydration strain' which is a time-dependent strain associated with the degree of hydration and represents the age dependence of creep strain, is proportional to the number of units of uncrystallized material remaining in the cement paste, which is decreasing. Therefore, a linear homogeneous Markov death process is chosen. Based on the above physical interpretation, the mean value and the variance of creep strain are expressed as follows (cf. Fig. 5.1).

$$\varepsilon(\tau) = \varepsilon_v(\tau) + \varepsilon_E(\tau) + \varepsilon_H(\tau) \tag{5.1}$$

$$\begin{aligned} E[\varepsilon(\tau)] &= E[\varepsilon_v(\tau)] + E[\varepsilon_E(\tau)] + E[\varepsilon_H(\tau)] \\ &= C_v\sigma\gamma \ln[(\tau+T)/T] + (\sigma/E)(1-e^{-\alpha\tau}) \\ &\quad + (C_H\sigma N_0/\lambda)e^{-\lambda\tau}(1-e^{-\lambda\tau}) \end{aligned} \tag{5.2a}$$

$$\begin{aligned} \mathrm{Var}[\varepsilon(\tau)] &= \mathrm{Var}[\varepsilon_v(\tau)] + \mathrm{Var}[\varepsilon_E(\tau)] + \mathrm{Var}[\varepsilon_H(\tau)] \\ &= C_v^2\sigma\gamma \ln[(\tau+T)/T] + (C_E\sigma/E)e^{-\alpha\tau}(1-e^{-\alpha\tau}) \\ &\quad + (C_H^2 N_0\sigma^2/\lambda^2)\{e^{-\lambda T}(1-e^{-\lambda\tau})[2-e^{-\lambda T}(1-e^{-\lambda\tau})] \\ &\quad - 2\lambda\tau e^{-\lambda(T+\tau)}\} \end{aligned} \tag{5.2b}$$

where ε = total basic creep strain, ε_v = viscous strain, ε_E = delayed-elasticity strain, ε_H = hydration strain, $\tau = t - T$ = time since loading, t = current time, T = age at loading, σ = applied stress, E = effective modulus of elasticity of the skeleton. Here $E[\cdot]$ and $\mathrm{Var}[\cdot]$ stand for the mean value and the variance, respectively. Also, C_v, C_E, C_H = material constants, N_0 = initial population of

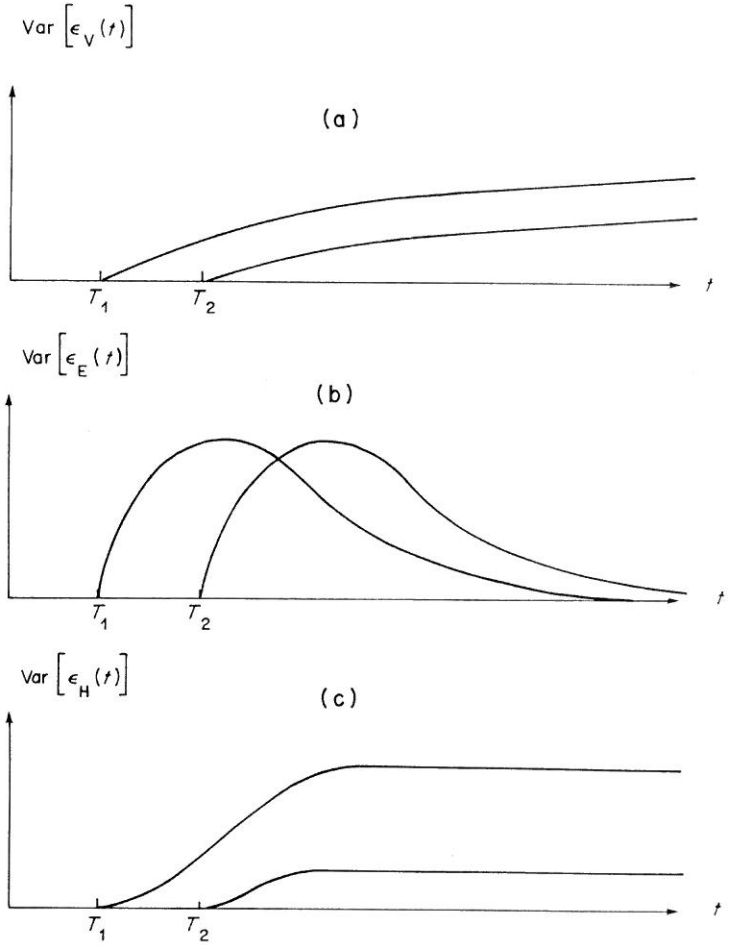

Figure 5.1 Stochastic creep model: variance functions of the component processes of the creep mechanism for two ages at loading (Cornell, 1964). Reproduced by permission of C. A. Cornell

potential unhydrated crystals, γ = proportionality constant to define the transition intensity of the non-homogeneous Poisson process, $\mu(t)$, i.e. $\mu(t) = \gamma\sigma/t$, $\alpha = \beta E C_E$, β = proportionality constant to define the transition intensity of the homogeneous Markov linear death process, $\nu(t)$, i.e. $\nu(t) = \beta\sigma_w(t)$, where $\sigma_w(t)$ is

the stress carried by the water, $\sigma_w(t) = EC_E\{W(t) - W(\infty)\}$, where $W(t)$ is the volume of water within the skeleton, and λ = rate of transition intensity of the Markov linear death process.

The form of the above mean function is similar to the following empirical formula of creep strain proposed by Hansen (1960) and Roll (1964).

$$\varepsilon(\tau) = C_1\sigma \ln[(\tau + T)/T] + C_2\sigma(1 - e^{-m\tau}) + C_3\sigma[(1 - g(T))/g(T)](1 - e^{-m\tau}) \quad \text{(Hansen)} \tag{5.3}$$

where $g(T)$ is a function to express the degree of hydration at the time of loading, C_1, C_2, C_3 = material constants dependent on mix proportions, etc., m = empirical constant.

$$\varepsilon(\tau) = C_1/\lambda(1 - e^{-\lambda\tau}) + \sigma C_2(1 - e^{-\alpha\tau}) + \sigma C_2(1 - e^{-100\alpha\tau}) \quad \text{(Roll)} \tag{5.4}$$

where C_1, C_2 = stress-dependent functions, α, λ = empirical constants. Empirical parameters involved in the model are obtained by a statistical regression analysis. Several directions of the extension of the model are also suggested. Among them are the effects of the non-linearity in stress, the dependence of parameters on mix composition, aggregate and curing conditions, the size of specimens, the environmental conditions such as temperature, and the time-varying loads.

In the work of Gabrielsen (1966), a Markov chain with continuous parameters is discussed to model stochastic processes of general stochastically viscoelastic materials. An infinitesimal transition probability matrix for a birth and death process which is non-homogeneous in time to represent the ageing effect is derived. The mean, variance, and covariance functions of the creep strain for simple materials are obtained as follows (cf. Figs. 5.2, 5.3). For a three-parameter solid,

$$\begin{aligned} E[J(t)] &= (1/E) + c\bar{N}(1 - e^{-\lambda t}); \\ \mathrm{Var}[J(t)] &= k^2 + c^2\bar{N}e^{-\lambda t}(1 - e^{-\lambda t}); \\ \mathrm{Cov}[J(s), J(t)] &= k^2 + c^2\bar{N}e^{-\lambda t}(1 - e^{-\lambda s}) \quad (0 \leqslant s \leqslant t) \end{aligned} \tag{5.5}$$

where $J(t)$ = creep compliance, t = time since loading, E = elastic modulus of the spring, c = a constant of proportionality between the counting process and the strain process, $\bar{N} = N/\bar{\sigma}$, where N = number of molecules contained in the damper at $t = 0$, and $\bar{\sigma}$ = number of applied unit stresses, i.e. $\bar{N}$ = total number of molecules available to be born with a unit load, λ = birth-rate at which molecules leave the damper, k = standard deviation of the elastic compliance of the spring. Cov[·] stands for the covariance function.

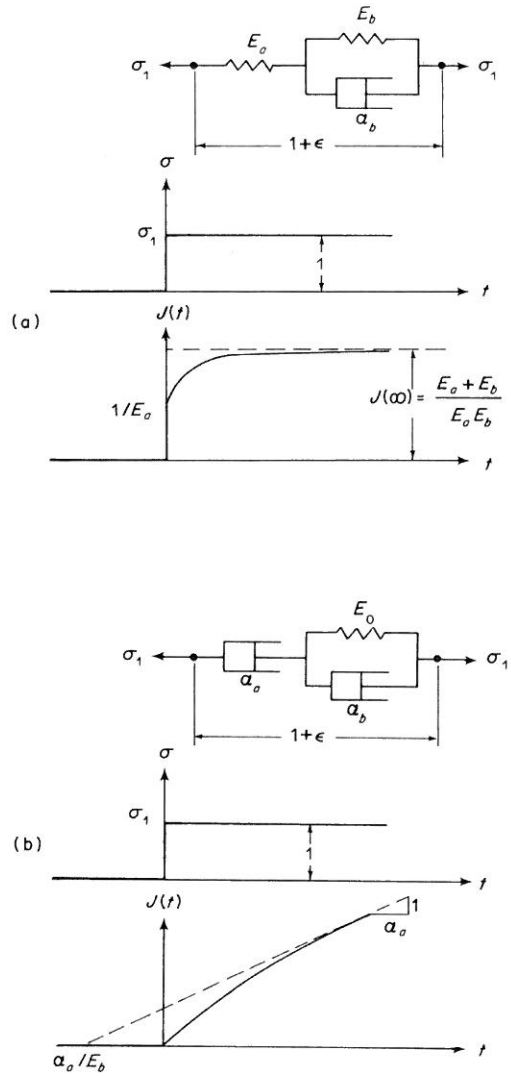

Figure 5.2 Viscoelastic models: (a) three-parameter solid response: (b) three-parameter fluid response (Gabrielsen, 1966). Reproduced by permission of C. A. Cornell

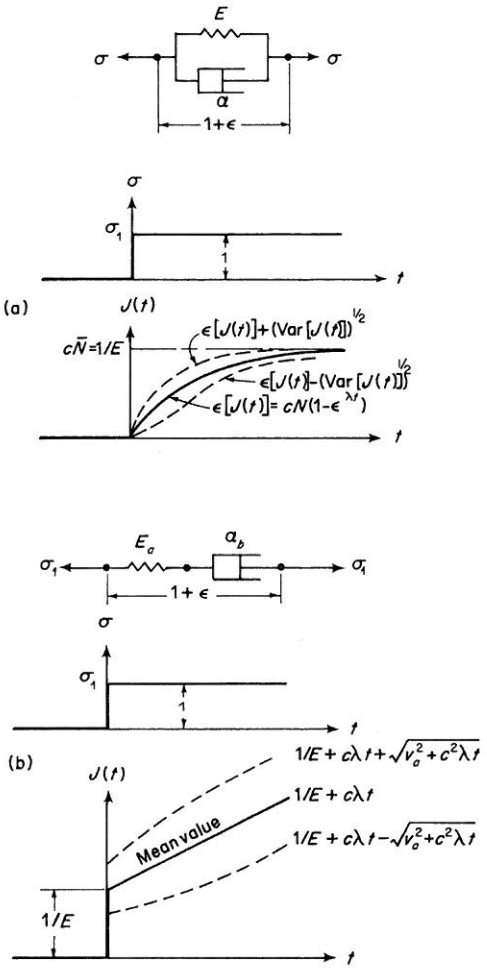

Figure 5.3 Stochastic models: (a) stochastic Kelvin solid response; (b) stochastic Maxwell fluid response (Gabrielsen, 1966). Reproduced by permission of C. A. Cornell

For a three-parameter fluid,

$$E[J(t)] = c_1\lambda_1 t + c_2\bar{N}(1-e^{-\lambda_2 t});$$

$$\mathrm{Var}[J(t)] = c_1^2\lambda_1 t + c_2^2\bar{N}e^{-\lambda_2 t}(1-e^{-\lambda_2 t});$$

$$\mathrm{Cov}[J(s),J(t)] = c_1^2\lambda_1 s + c_2^2\bar{N}e^{-\lambda_2 t}(1-e^{-\lambda_2 s}) \quad (0\leqslant s\leqslant t) \tag{5.6}$$

where C_1 = proportionality constant between the counting process and the strain process of the viscous damper, C_2 = proportionality constant for the kelvin solid, and subscripts 1 and 2 indicate viscous damper and Kelvin solid respectively. Other notations are the same as Eq. (5.5).

Application of this model to bending problems of homogeneous reinforced concrete (RC) beams is also shown in Gabrielsen (1966).

The model used by Benjamin *et al.* (1965) is a simplified version of the above models. Creep strain is decomposed into only two parts, i.e. strains due to viscous flow and delayed elasticity. The Markov birth process is employed to represent both the viscous flow and the delayed-elastic effects. The reason a Markov birth process is chosen for the delayed-elastic part instead of a Markov death process as in Cornell (1964) is that the process related to the delayed elasticity is assumed to be proportional to a 'population' of fluid squeezed out from within the elastic skeleton, the amount of which is increasing. The mean, variance, and covariance functions of creep strain are expressed as follows:

$$\varepsilon(t) = \varepsilon_v(t) + \varepsilon_E(t) \tag{5.7}$$

$$E[\varepsilon(t)] = E[\varepsilon_v(\tau)] + E[\varepsilon_E(\tau)]$$

$$= \sigma C_v\gamma\ln[(\tau+T)/T] + [\sigma/E(t)](1-e^{-\alpha\tau}) \quad (\tau\geqslant 0);$$

$$\mathrm{Var}[\varepsilon(\tau)] = \sigma C_v^2\gamma\ln[(\tau+T)/T] + [\sigma C_E/E(T)]e^{-\alpha\tau}(1-e^{-\alpha\tau}) \quad (\tau\geqslant 0);$$

$$\mathrm{Cov}[\varepsilon(\tau),\varepsilon(\tau')] = \sigma C_v^2\gamma\ln[(\tau+T)/T] + [\sigma C_E/E(\tau)]e^{-\alpha\tau'}(1-e^{-\alpha\tau})$$

$$(\tau'\geqslant\tau\geqslant 0) \tag{5.8}$$

where notations are the same as those of Eqs (5.1) and (5.2).

Then, using this creep model, the mean and variance functions of the deflection of any point on a RC beam at any time are derived. Also obtained are the spatial and temporal covariance functions by which one can take advantage of an early observation of the creep deflection to alter the prediction of later deflections and to reduce the variance of these predictions. Reformulation of the results with an extension to time-varying loads is also shown.

In the model of Chow and Shah (1971), a linear homogeneous Markov death process is used. The creep mechanism is decomposed into four parts, i.e. the viscous flow, the delayed elasticity, the seepage, and the localized fracture, following the deterministic model of Roll (1964) which better fits test data than Hansen's (1960) model (cf. Fig. 5.4). Each part is modeled by a linear homogeneous Markov death process from the following reasoning. The cement paste, in

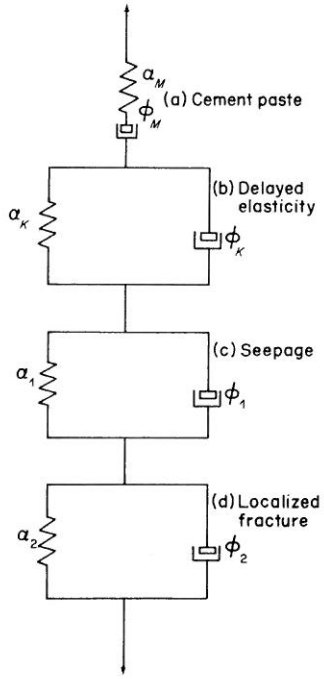

Figure 5.4 Mechanical model representing the various deformation mechanisms of concrete (Chow and Shah, 1971). © 1971. Reprinted by permission of John Wiley & Sons Ltd

which the aggregate and crystalline particles of cement are suspended, is a highly viscous liquid. The viscosity of the paste increases as hydration continues. When constant sustained compressive stress is applied to concrete, a portion of potential creep due to viscous flow is introduced. This portion of creep proceeds at a decreasing rate. The decrease in creep rate at increasing time under the sustained load is due to the gradual increase in viscosity of the paste as hydration progresses. Considering that the rate of creep at a certain time is linearly proportional to the amount of the potential creep remaining, the viscous flow part of creep is modeled as a linear homogeneous Markov death process. When concrete is loaded by a constant sustained load, at first the cement paste and free water carry part of the load. The part carried by the paste is gradually transferred to the skeleton of the cement crystals and to the aggregate as time increases.

Another part of the load which is carried by the free water is transferred to the skeleton of the cement crystals and to the aggregate with the movement of the free water molecules. The loads which are transferred from the paste and the free water cause the delayed-elastic effect. A portion of creep is thus caused by this delayed-elastic effect. The creep rate caused by the delayed-elastic effect depends on the stress remaining in the paste and free water, and therefore it decreases with time. Considering that the delayed elasticity is a function of the stress remaining in the paste and free water, a linear homogeneous Markov death process is chosen to model this process. The portion of creep due to seepage is assumed to be caused by the movement of water from the colloidal cement gel and free water. Application of a constant sustained compressive stress to concrete tends to squeeze the water out from the gel pore into the capillaries or into other pores and towards the surface of the concrete where the water may eventually be evaporated. After water has moved out, voids may exist into which the concrete mass can move, and cause seepage creep to occur. The rate of this process depends on the decreasing amount of pore water or gel water which is left in the concrete. Similar to the two previous factors, the linear homogeneous Markov death process is chosen for this process. Finally, a portion of creep of concrete is caused by the localized fracture of concrete, when it is subjected to constant sustained compressive stress. The creep due to localized fracture depends on the applied stress and time. Assuming that the rate of creep due to localized fracture is proportional to the amount of potential internal microcracking, the creep rate depends on the decreasing amount of unfractured materials of the concrete. If creep is a function of unfractured material still available in the concrete, a linear homogeneous Markov death process can be used for this process. Then, the total creep is expressed as a sum of the above four processes. The mean and variance functions of creep strain are obtained as follows:

$$E[\varepsilon(t)] = \sum_{i=1}^{4} (C_i/\mu_i)e^{-\mu_i\tau}(1 - e^{-\mu_i\tau}) \qquad (\tau \geqslant 0, T \geqslant 0);$$

$$\mathrm{Var}[\varepsilon(t)] = \sum_{i=1}^{4} (C_i^2/\mu_i^2)\{e^{-\mu_i T}(1 - e^{-\mu_i})$$
$$[2 - e^{-\mu_i T}(1 - e^{-\mu_i\tau})] - 2\mu_i e^{-\mu_i(T+\tau)}\}$$
$$(T \geqslant 0, \tau \geqslant 0) \qquad (5.9)$$

where $\varepsilon(t)$ = total basic creep strain (compliance), $\tau = t - T$ = time after load is applied, t = current time, T = age of concrete at the time of loading, C_i = constant dependent on the applied stress, and μ_i = linear death rate of the ith factor.

The mean function is basically identical to the empirical deterministic formula of creep strain proposed by Roll (1964). The empirical constants involved in the model are obtained by a trial-and-error method, rather than a non-linear regression analysis, so that the mean function fits the test data (cf. Fig. 5.5).

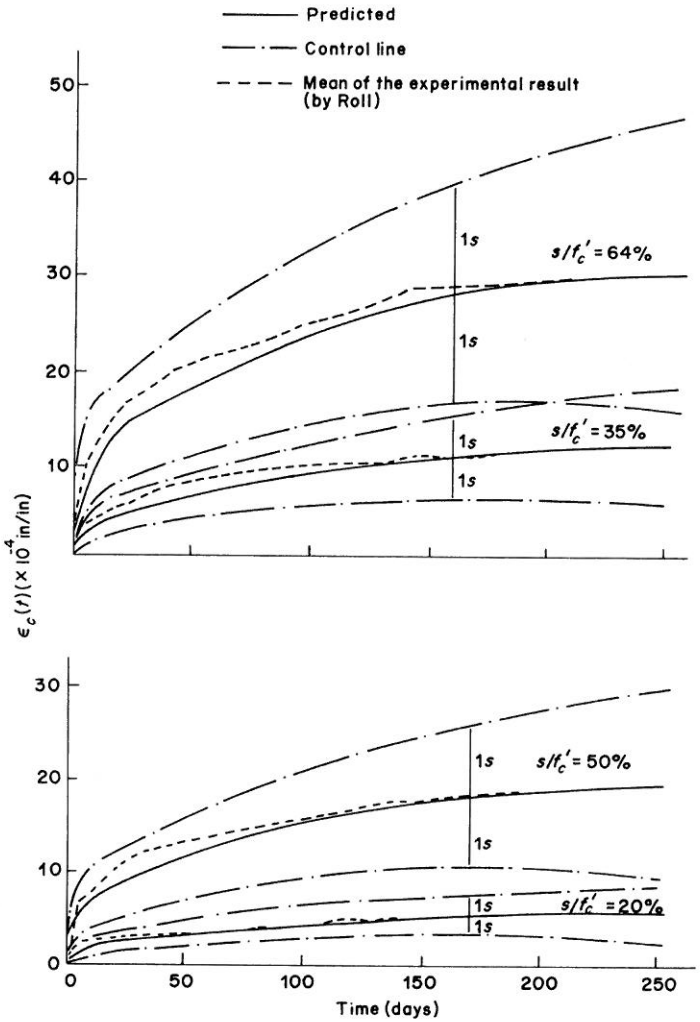

Figure 5.5 Stochastic creep model: comparison of creep curves (mix 1:1 from Roll, 1964) (Chow and Shah, 1971) (1 in = 25.4 mm). © 1971. Reprinted by permission of John Wiley & Sons Ltd

5.3.2 Gamma process model

Çinlar *et al.* (1977) proposed a stochastic model of basic creep using the local gamma process. Four random processes may be considered as a candidate for a stochastic creep model, i.e. Gaussian, stable, Poisson, and gamma processes. The main reason for the choice of these four processes is that their distributions are infinitely divisible, i.e. sum of many variables of these distributions has the same distribution as the distribution of each variable. The main point of this work is to formulate this infinite divisible condition in an explicit form, which is inevitable in constructing a stochastic creep model. Among these four distributions, only the local gamma process satisfies the necessary requirements. The reason is described in the following.

Assuming that the stochastic process involved in one-directional creep phenomenon under unit compression is increasing, bounded, and of independent increments, statistically tractable processes with such characteristics are the Gaussian, stable, Poisson, and gamma processes. Gaussian processes are excluded because creep is increasing. Stable processes are excluded because the only increasing ones have index less than 1 and such stable processes have infinite expectations. Poisson processes are excluded because creep should have a continuous distribution (and because the coefficient of variation, which is equal to the square root of the mean, becomes negligible of large members). An ordinary gamma process is excluded because of the obvious non-stationary of creep. However, local gamma processes are capable of handling non-stationary and yet are statistically tractable. Also, among continuous distributions, after excluding the Gaussian and exponential distribution, the gamma distributions are the easiest to deal with and are known to fit a wide range of experimental distributions. After transformation of a local gamma process into an ordinary gamma process, the mean and variance functions of creep strain (creep compliance) $J(s)$ are obtained as follows:

$$E[J(s)] = (a_0/b_0)z; \qquad \mathrm{Var}[J(s)] = (a_0/b_0^2)z; \qquad z = (1/n)s^n \tag{5.10}$$

where a_0 and b_0 are the shape and scale parameters for an ordinary gamma process which are dependent on the age at loading. Also, s is the time elapsed since the load is applied and n is an empirical constant. The mean function of this model is equivalent to the double power law (Bažant and Osman, 1976). The parameters involved in the model are obtained by the method of moments and the method of maximum likelihood. A comparison with test data is shown in Fig. 5.6. The extension of the above-mentioned model for the case of a unit uniaxial stress to the case of a variable stress history within the linear response range is also given by Çinlar and Bažant (1979), in which the principle of superposition in probabilistic terms is discussed.

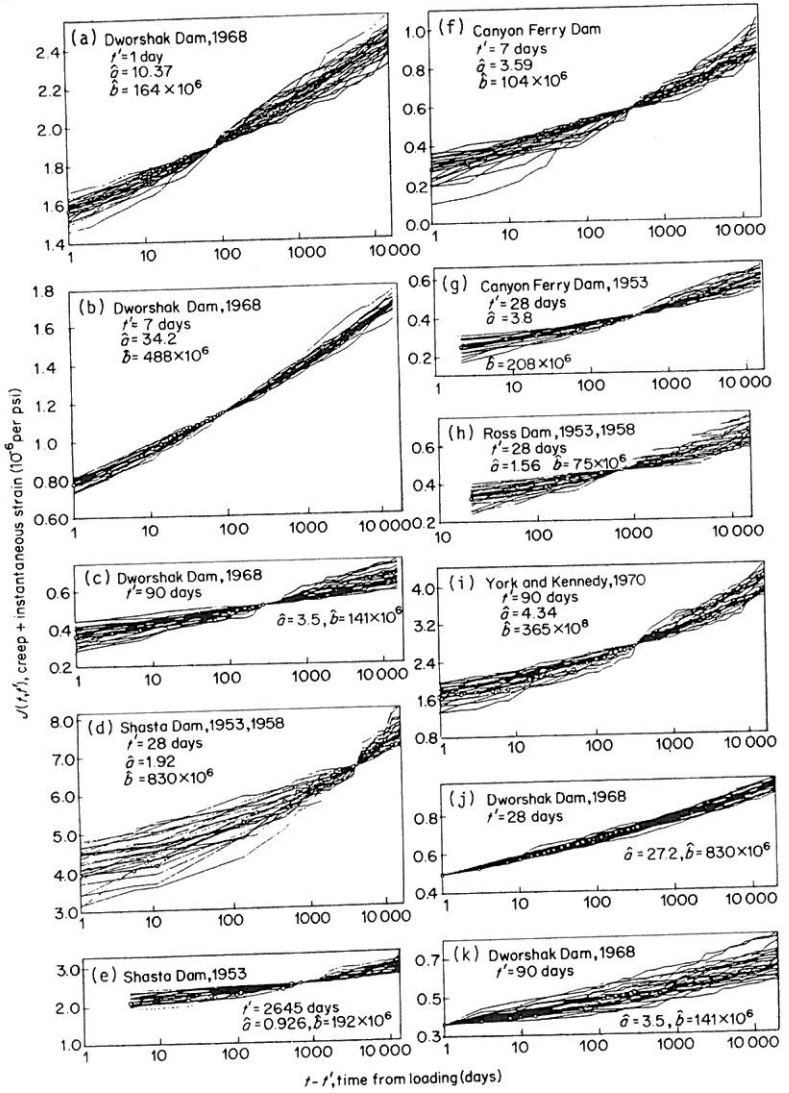

Figure 5.6 Stochastic creep model: Monte Carlo simulation with non-stationary gamma process, compared with test data (Çinlar *et al.*, 1977) (1 psi = 6.89 kPa). Reproduced by permission of ASCE

5.3.3 White noise process model

Ditlevsen (1982a) proposed a stochastic model for uniaxial creep using a white noise process. This model yields a stochastic white-noise-type constitutive equation for uniaxial strain and stress. The reason a white noise process was chosen is that it is 'the simplest possibility of consistent modeling'. In the mean, this model is consistent with usual linear viscoelastic theory. The outline of the model is as follows. The creep strain in the direction of the x-axis at r is expressed as

$$\varepsilon(r,t)=\int_{\tau=0}^{t}\int_{\sigma(r,\tau)}^{\sigma(r,\tau)+\mathrm{d}\sigma(r,\tau)} S(r,t,\tau,u)\,\mathrm{d}u \tag{5.11}$$

where $\varepsilon(r,t)$ = creep strain in the direction of the x-axis at r, $\sigma(r,t)$ = 'normal-to-cross-section' stress history with $\sigma(r,t)=0$ for $t\leqslant 0$, t = current time; $r=(x,y,z)$ where x is the axial direction, and y and z are cross-section coordinates; $S(r,t,\tau,u)$ is a second moment white noise process (wide-sense white noise process) in the geometrical (r), time (τ), and stress (u) space, i.e.

$$E[S(r,t,\tau,u)]=K(t,\tau);\qquad \mathrm{Cov}[S(r_1,t_1,\tau_1,u_1),S(r_2,t_2,\tau_2,u_2)]$$
$$=c(t_1,t_2,\tau_1)\delta(\tau_2-\tau_1)\delta(u_2-u_1)\delta(r_2-r_1) \tag{5.12}$$

where $K(t,\tau)$ = creep function of usual linear viscoelasticity theory, $c(t_1,t_2,\tau_1)$ = suitable covariance function, and $\delta(\cdot)$ = the Dirac delta function. Then, the mean and covariance functions of creep strain are expressed as

$$E[\varepsilon(r,t)]=\int_{\tau=0}^{t}K(t,\tau)\,\mathrm{d}\sigma(r,\tau);$$
$$\mathrm{Cov}[\varepsilon(r_1,t_1),\varepsilon(r_2,t_2)]=\delta(r_2-r_1)\int_0^{t_1}c(t_1,t_2,\tau)|\mathrm{d}\sigma(r_1,\tau)|$$
$$(t_1\leqslant t_2) \tag{5.13}$$

With a unit average normal stress applied to time T and kept constant for $t\geqslant T$, the mean and covariance functions are:

$$E[\varepsilon(t)]=K(t,T)\qquad (t\geqslant T);$$
$$\mathrm{Cov}[\varepsilon(t_1),\varepsilon(t_2)]\geqslant(1/LA)c(t_1,t_2,T)\qquad (t_2\geqslant t_1\geqslant T) \tag{5.14}$$

where L and A stand for the length and the area of a concrete column respectively. Equations (5.13) and (5.14) indicate that this model has a general form which includes the models based on the Markov process. In fact, it can be adapted to any model leading to explicit expressions for the creep function $K(t,\tau)$ and the covariance function $c(t_1,t_2,\tau)$, although it is necessary to choose processes with

non-negative sample functions. As applications of the above models, second-moment representations for several different types of beam-column problems are shown. Further application of the above white noise model is discussed by H. Madsen and Ditlevsen (1980). As the references for the part of the algorithm used in the above works and its applications, see the works by K. Madsen (1979, 1980). Also, the above model for uniaxial creep has recently been generalized by Ditlevsen (1982b) for triaxial creep in a statistically isotropic case. This model gives a random strain tensor for a given deterministic stress tensor history. See also Ditlevsen (1984) for related topics.

5.3.4 Remarks

As stated above, there are several probabilistic (stochastic) constitutive models. Those constitutive models are based on the physical micromechanism of creep of concrete. However, the final judgement in choosing a stochastic process to be employed in the model depends on how the micromechanism of creep is interpreted and is not determined uniquely. So far, the method of developing a probabilistic model appears to be phenomenological and qualitative. It is desirable to make quantitative comparison of these models for a given problem. A good constitutive model must be easy to handle as well as consistent with the mechanism of the phenomenon.

For the definition of terms on probability and stochastic processes, and also for the methods of prediction of empirical material parameters involved in models, Benjamin and Cornell (1970), Feller (1971), Çinlar (1975), Ditlevsen (1981), and Lind *et al.* 1985) may be consulted. Also, a detailed description on probabilistic approach to deformations of concrete is given by Çinlar (1982). See also Krenk (1986).

5.4 STATISTICAL ASPECTS OF CREEP AND SHRINKAGE

In the previous sections of this chapter, the effect of internal physical mechanisms of creep on the statistical variation of creep has been discussed. Even if other factors of the statistical variation are all eliminated, this effect will remain unchanged. In addition to the internal mechanism factor, other factors of variation also exist in materials and environmental conditions, which are usually more influential than the internal factors. Even in the laboratory experiment, it is possible that the statistical variation (scatter) of creep and shrinkage data due to such factors cannot completely be eliminated. Therefore, we might well realize that the creep and shrinkage data reported in the literature are influenced by those factors to some extent, and some statistical scatters are included. In this section, some experimental works to investigate the scatter in the data of creep and shrinkage are reviewed. Then, an overview of statistical methods to predict the scatter of creep and shrinkage is given.

5.4.1 Experimental study of creep and shrinkage

A couple of experimental works to investigate the magnitude of scatter and the influence factors of creep and shrinkage have recently been reported. Alou and Wittmann (1982) studied the shrinkage of concrete to estimate the final shrinkage by extrapolation. Cylindrical specimens between 100 and 500 mm in diameter of two different concrete mixes were used. The specimens were set under 18° C and 65 per cent relative humidity for four months during measurement. It is reported that variation in the measured shrinkage was caused by the precision of the measuring technique during the first few days. After one month of drying, then, the scatter of the material properties become dominant. It is also reported that, the CEB–FIP code prediction is an underestimate. Since shrinkage of a concrete structure is influenced by the stochastic variables involved in the regional climate, such as temperature, wind speed, and humidity, the variation observed in a controlled laboratory test is a lower bound. Reinhardt *et al.* (1982) reported the variability of drying creep and shrinkage. Factors held constant were the specimen size and the mix proportions. Data were measured for 300 days. Load for creep was 20 and 40 per cent of the compressive strength. Cornelissen (1979, 1982) also reported the test result on the scatter of creep due to variations of concrete composition (water–cement ratio, aggregate-cement ratio). The effect of alternating temperature and relative humidity was also examined. Factors held constant were the size and shape of specimens, the type and grading of aggregate, the curing conditions, the load and age at loading, and the load duration.

It is desirable to accumulate these kinds of data, because it appears that there are only a few references on this subject. From a practical point of view, long-term observation of actual concrete bridges is also necessary and such data should also be accumulated. Jávor (1982, 1984, 1985) may be consulted for the method and the data of long-term observation of actual bridges. A method of measuring long-term strains in concrete using a microcomputer was reported recently (Hirst, 1983) and this kind of approach will provide accurate and continuous data to be used to make a mathematical model.

As this report goes to press, a large series of concrete shrinkage tests which can be used for statistical purposes has just been reported (Wittmann *et al.*, 1987). The series involves two groups of 36 identical cylindrical specimens, with a diameter of 83 mm for group 1 and 160 mm for group 2. Statistical analysis of shrinkage strains and strain rates is presented and the goodness of fit by normal distribution, log-normal distribution, and gamma distribution is analysed. Correlations between the values at various times are determined. The study reveals only the intrinsic randomness of the shrinkage process (along with measurement errors) and omits the superimposed uncertainties due to randomness of environment and to prediction uncertainties in the influence of material composition, curing, and other factors. Some of the results of measurements are plotted in Figs 5.7–5.10. The following observations can be made from these results.

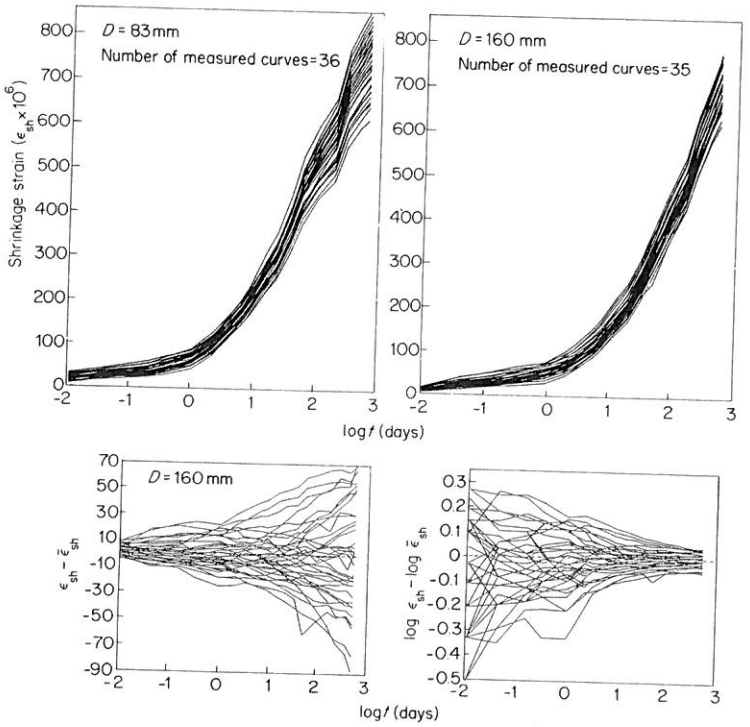

Figure 5.7 Shrinkage curves for individual cylinders, and deviations of strain from mean strain and of log-strain from mean log-strain (after Wittmann *et al.*, 1987)

While the standard deviation of shrinkage values of all specimens increases with time, their coefficient of variation decreases and appears to reach a constant value of about 8.5 per cent for the cylinders of smaller diameter, and about 6 per cent for the cylinders of larger diameter. The observed means for the set of all specimens have corresponding coefficients of variation of only 1.4 per cent and 1.0 per cent. The values 8.5 per cent and 6 per cent are relatively small, which reveals that the shrinkage process *per se* is not a major source of uncertainty. Rather it is the various random, poorly controlled, or unknown influences which make shrinkage predictions in practice as uncertain as they are known to be.

The distribution of shrinkage values at a fixed time may be approximately considered to be normal (Gaussian), as confirmed by Figs. 5.8 and 5.9. However, the log-normal distribution and the gamma distribution fit the observed frequency density distributions (Fig. 5.9) at least as well, and they are both

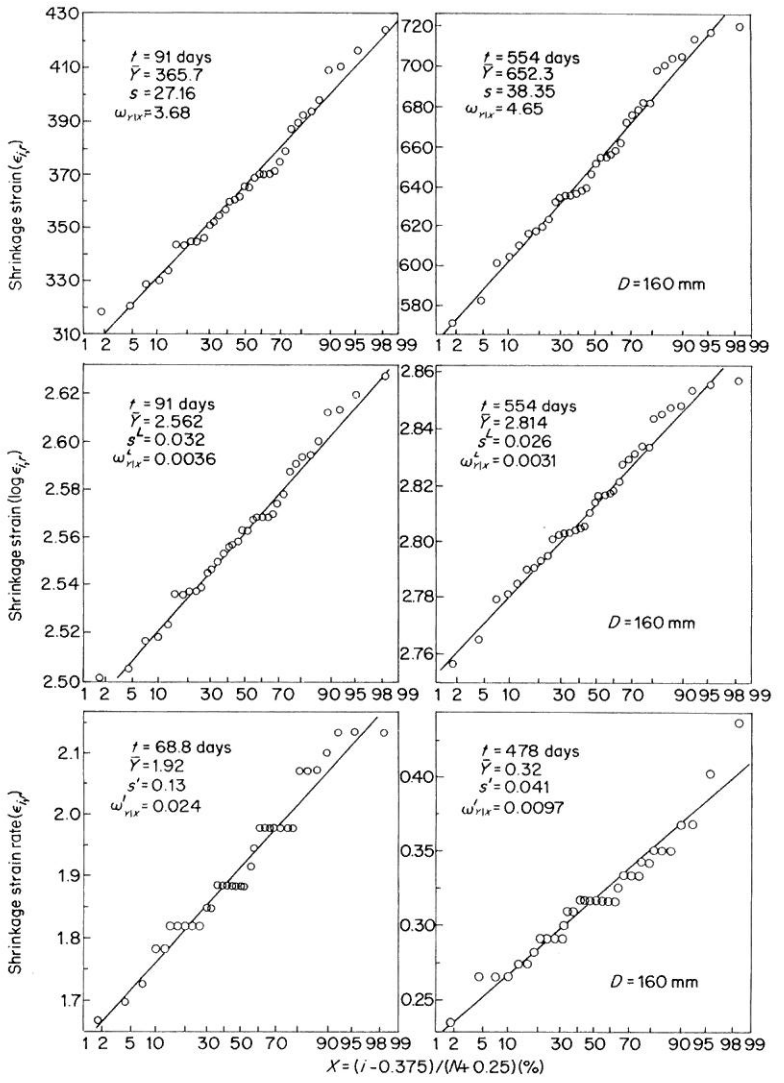

Figure 5.8 Cumulative distributions of shrinkage strain, log-strain, and strain rate (after Wittmann *et al.*, 1987)

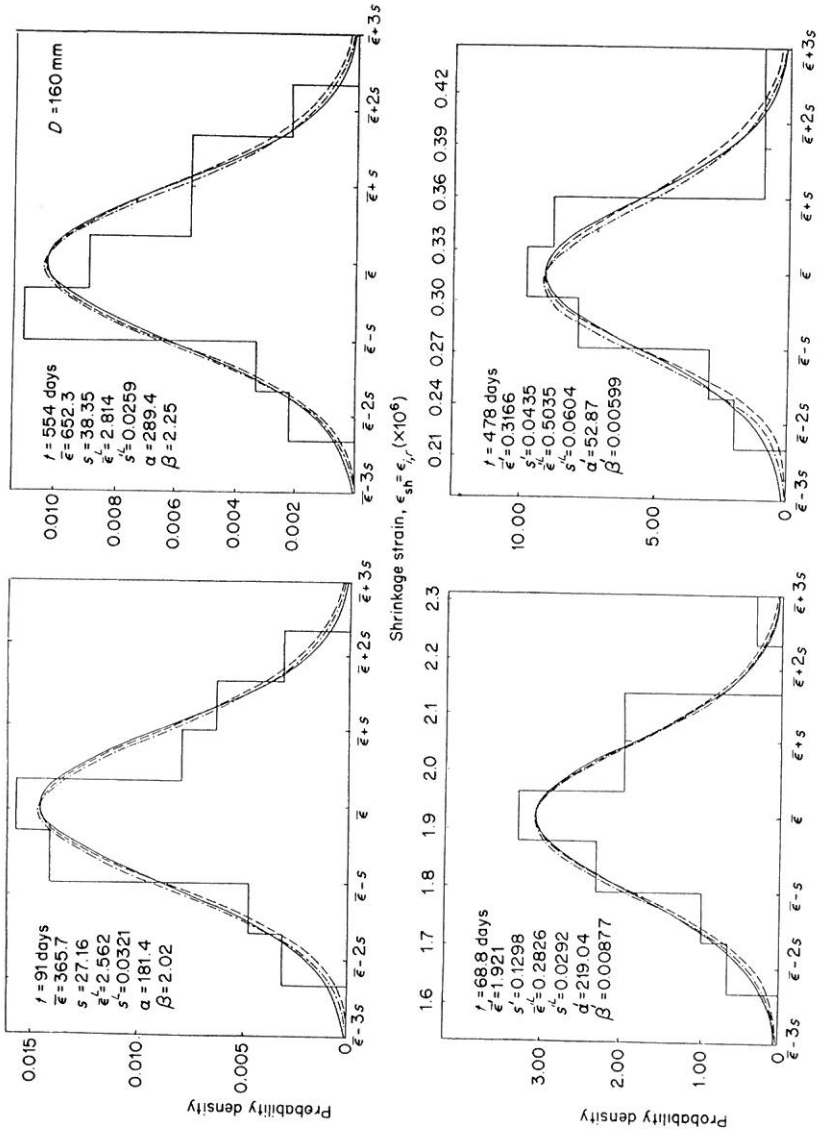

Figure 5.9 Probability density distributions of shrinkage strain and shrinkage strain rate (after Wittmann *et al.*, 1987)

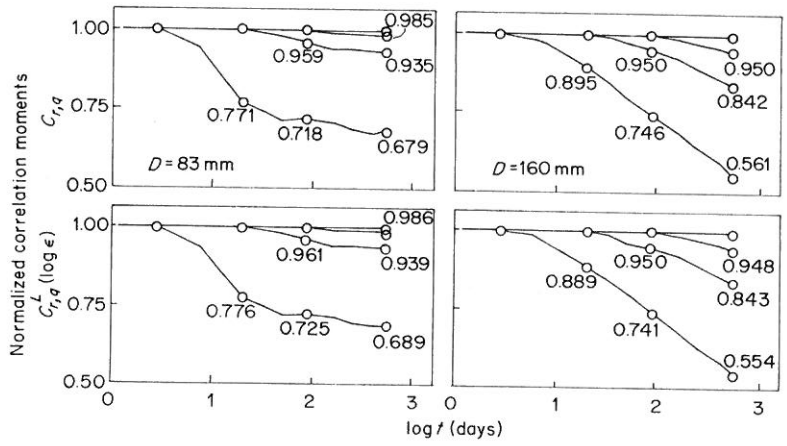

Figure 5.10 Normalized correlation moments of shrinkage strains at two different times (after Wittmann *et al.*, 1987)

obtained as very close to the normal distribution. The reason for this closeness is that the coefficient of variation is relatively small. There are, nevertheless, small systematic deviations from the normal distribution. All the observed distributions of shrinkage strain are slightly asymmetric and have a positive skewness. This means that they are all skew to the right, i.e. have a longer tail towards the high values and a shorter tail towards the small values. The positive value of skewness confirms that asymmetric distributions such as log-normal or gamma are better than the normal distribution. This agrees with the fact that negative shrinkage values are impossible. The log-normal and gamma distributions, unlike the normal distribution, do not permit negative values. Another deviation from the normal distribution is due to the fact that all the observed distributions are slightly platykurtic (i.e. have a flatter top and shorter tails than the normal distribution). This is revealed by the fact that the kurtosis coefficient is systematically less than 3 (which is the value of kurtosis for normal distribution).

The observed cumulative distributions of shrinkage rates (Fig. 5.8) show somewhat larger deviations from the normal distribution, with a more pronounced skewness. Mostly they deviate upward from the straight line at the right end, which indicates skewness to the right. The skewness coefficients for the shrinkage rates are larger than those for the shrinkage values. The observed cumulative distributions of log-strain and the frequency distributions of the observed rates also reveal skewness. Thus, the shrinkage rates are described somewhat better by the gamma or log-normal distributions than by the normal distribution,

although the normal distribution seems also acceptable empirically (theoretically, though, it is objectionable because it permits negative shrinkage rates which are impossible).

The deviations of a single-specimen shrinkage from the group mean observed at various times are correlated. For short time intervals the correlation is high, and for long intervals the correlation significantly decreases (Fig.5.10). The correlation coefficient of these deviations is about 0.6 for the time interval from 3 days to 550 days. The correlation of the deviations of the single-specimen shrinkage rates from the group mean is much weaker (Fig. 5.10).

In agreement with the foregoing observation, a specimen whose shrinkage is on the high (or low) side of the mean is likely to remain on the high (or low) side for short times, but less likely for a longer time. This is illustrated by the histories of shrinkage deviations shown in Fig. 5.7. The standard deviation of the individual specimen shrinkage values from the smoothed shrinkage curve of the same specimen is much smaller than (about one-third of) the standard deviation of the individual shrinkage values from the mean for the group of all specimens.

5.4.2 Statistical extrapolation of creep and shrinkage by regression

The variation of creep data and its influence on deterministic creep models were reported by Bažant and Panula (1978, 1979, 1980). Test data for 80 different countries from various laboratories throughout the world, consisting of over 800 experimental curves and over 10 000 data points have been analysed statistically. These data has also been organized in a computerized data base (Zebich and Bažant, 1981). It has been shown that, if no measurements for a given concrete are made, the uncertainty of its creep and shrinkage prediction on the basis of the chosen mix parameters and the chosen design strength is enormous (Bažant and Panula, 1980). For example, the prediction errors that are expected with a 10 per cent probability (90 per cent confidence limits) are 31 per cent for the BP model (Bažant and Panula, 1978, 1979), 63 per cent for the ACI 1971 model (ACI Committee, 1971, 1982), and 76 per cent for the CEB–FIP (1978) Model which uses the model proposed by Rüsch *et al.* (1973). An important conclusion from the above works is that a creep prediction formula for a design code must indicate the magnitude of scatter expected from using the formula. As in the CEB–FIP Model Code, it is desirable for a design code to indicate the extreme values, or the scatter around the mean value, of various material parameters used in concrete. So far, only the statistical distribution of the strength of material is taken into account. The statistical distribution of other material properties, e.g. creep and shrinkage of concrete should also be taken into account.

Statistically analysing creep data, Jordaan (1980, 1983) indicated that gauge, temperature and humidity variation are the main factors of stochastic variation of creep data, and creep of a macroscopic specimen at constant temperature and humidity is not a stochastic process in the sense that creep curves exhibit

negligible scatter about the mean of the particular curve being measured. Also suggested was the possibility of a Bayesian approach to deal with uncertainty of the magnitude of creep.

A statistical comparison of several deterministic models for the prediction of creep and shrinkage of concrete with creep data available in the literature was also reported by Bažant and Zebich (1983). The models were algebraically transformed into a linearized form, and statistical regression analysis was then carried out. The outline of the linear regression analysis is presented in the following. Prediction formulas for creep and shrinkage may be transformed into a linear form as follows:

$$y = a + bx + e \tag{5.15}$$

where x and y are the transformed independent and dependent variables, b is the slope, a is the y-intercept, and e is the error. Transformed formulas and their linear regression statistics for test data are summarized in Table 5.1. Although the scatter is large for all models, it is reported that the BP model (Bažant and Panula, 1978, 1979) performs distinctly better than the ACI and the CEB–FIP (1978) models (cf. Figs 5.11–5.12). In Figs 5.11 and 5.12, the resulting regression line, as well as the 90 per cent confidence limit for the mean predictions and for the individual data points, are shown as straight lines. It seems that more adequate

Table 5.1 Linear regression statistics of test data (Bažant, and Zebich, 1983). Reproduced with permission © 1983 Pergamon Journals Ltd.

		x	y
(a)	Basic creep		
	BP model (1)	$\phi_1(t'^{-m}+\alpha)(t-t')^n$	$E_0 J(t,t')-1$
	BP model (2)	$n\log(t-t')$	$\log[(J(t,t')E_0-1)/(\phi_1(t'^{-m}+\alpha)]$
	ACI model	$C_u[1+10(t-t')^{-0.6}]^{-1}$	$E(t')J(t,t')-1$
	CEB model	$\phi_d\beta_d(t,t')+\phi_f[\beta_f(t)-\beta_f(t')]$	$E_{28}J(t,t')-E_{28}/E_c(t')-\beta_a(t')$
(b)	Shrinkage		
	BP model	$\log(\tau_{sh}/\hat{t})$ $(\hat{t}=t-t_0)$	$\log[(\varepsilon_\infty/\varepsilon_{sh})^2-1]$
	ACI model	$\log(55)-\log(\hat{t})$	$\log[(0.0078/\varepsilon_{sh})-1]$
	CEB model	$\log[\beta_s(t)-\beta_s(t_0)]$	$\log(\varepsilon_{sh}/\varepsilon_{so})$

		$\bar{x}$	$\bar{y}$	s_x	s_y	a	b	s_b	$s_{y\|x}$	r
(a)	Basic creep									
	BP model (1)	0.495	0.464	0.351	0.306	0.019	0.999	0.005	0.304	0.820
	BP model (2)	2.559	2.739	1.713	1.916	0.180	1.062	0.003	1.920	0.933
	ACI model	0.630	0.520	0.335	0.521	−0.109	0.822	0.004	0.522	0.521
	CEB model	1.703	−1.004	0.862	0.173	−2.107	−0.458	0.005	0.173	0.265
(b)	Shrinkage									
	BP model	1.423	1.484	2.855	1.912	0.240	0.899	0.004	1.915	0.870
	ACI model	−0.495	0.166	1.973	0.185	0.411	0.044	0.005	0.185	0.479
	CEB model	−0.154	−0.204	0.866	0.459	−0.050	0.116	0.012	0.460	0.146

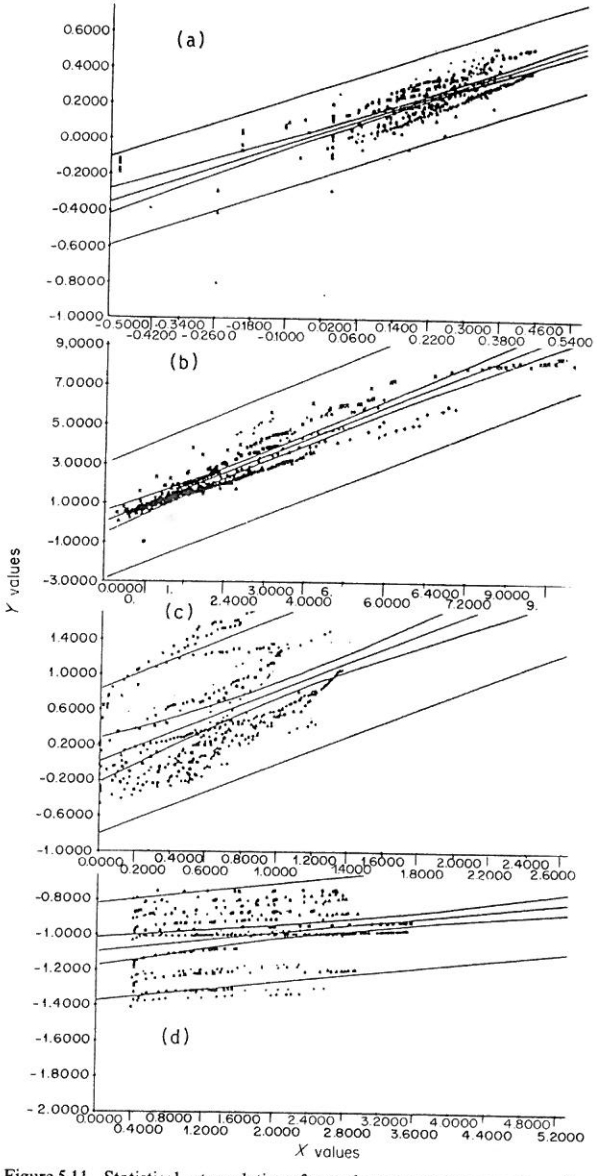

Figure 5.11 Statistical extrapolation of creep by regression: comparison of various prediction models for basic creep with existing test data: (a, b) BP model; (c) ACI model; (d) CEB model (Bažant and Zebich, 1983). Reprinted with permission from Z. P. Bažant and S. Zebich, Statistical linear regression analysis of prediction models for creep and shrinkage, *Cement and Concrete Research*, **13**(6), Nov., 869–76. © 1983 Pergamon Journals Ltd

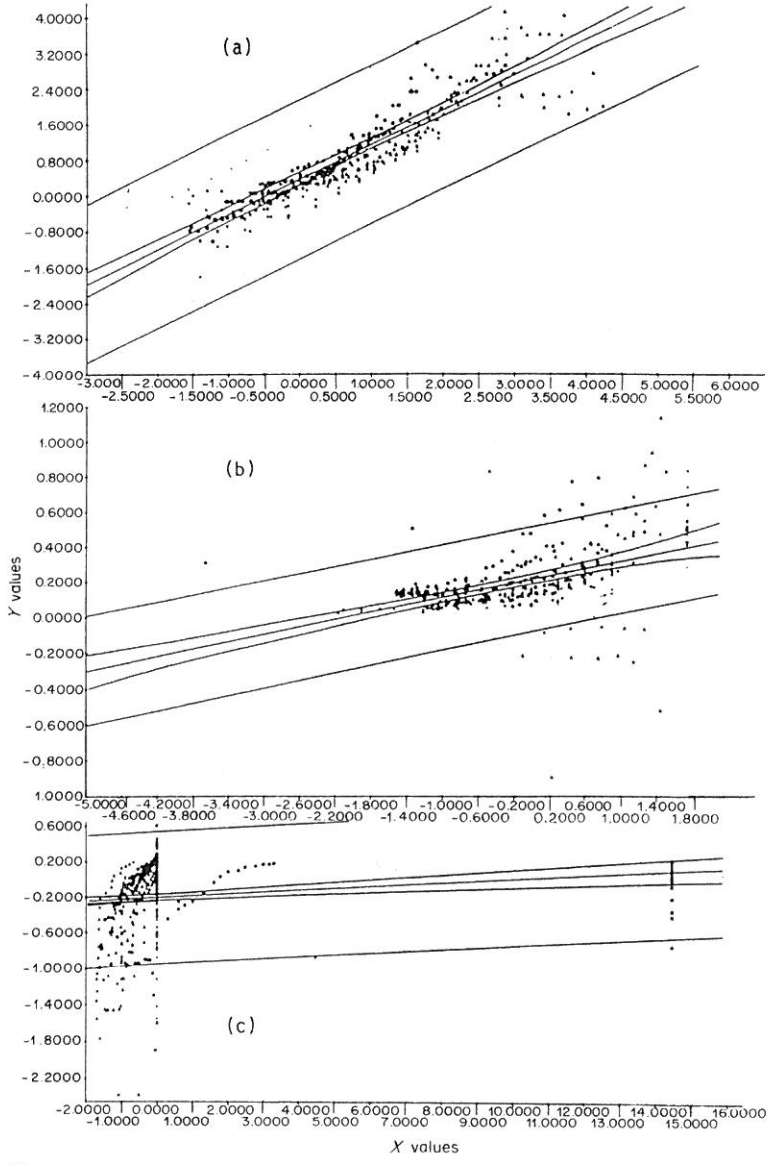

Figure 5.12 Statistical extrapolation of shrinkage by regression: comparison of various prediction models for shrinkage with existing test data: (a) BP model; (b) ACI model; (c) CEB model (Bažant and Zebich, 1983). Reprinted with permission from Z. P. Bažant and S. Zebich, Statistical linear regression analysis of prediction models for creep and shrinkage, *Cement and Concrete Research*, **13**(6), Nov., 869–76. © 1983 Pergamon Journals Ltd

data are necessary for the regression analysis in Fig. 5.12(c). Note that, in this statistical model, the errors are assumed to be independent from data point to data point for different test specimens but also for different observation times for each specimen. The independence assumption for errors for one specimen can be questioned and some of the plots in Fig. 5.11 show such points on straight lines parallel to the mean regression line. An extended model could then be

$$y_{ij} = a + bx_j + c_i + \varepsilon_{ij} \tag{5.15a}$$

where now $a + c_i$ is the intercept for the ith specimen, c_i is independent from test specimen to test specimen, j refers to time, and errors ε_{ij} are mutually independent. A hypothesis of $c_i = 0$ can then be tested to show if Eq. (5.15) is sufficient.

Recently, a large series of data on carefully controlled shrinkage tests of concrete involving groups of large numbers of identical specimens has been reported (Bažant *et al.*, 1985b, c, 1987). The summary of this study is given as follows.

The data are used to compare existing shrinkage formula in the ACI (ACI Committee, 1971, 1982), the CEB–FIP (1978) and the BP (Bažant and Panula, 1978; Box *et al.* 1978) models. The best agreement is obtained for the BP model. Assuming that only the measured data for a certain initial period are known, predictions are made for long times and compared with the subsequently observed shrinkage strains. In this manner, various possible statistical regression models are examined and compared. Best predictions are obtained when the shrinkage formula is fitted to test data using non-linear optimization, and then linear regression in transformed variables is used to obtain the confidence limits for long-time predictions (cf. Fig. 5.13). From this study, the following conclusions have been reported.

1. The shrinkage data used, which appear to represent the largest statistical set of data obtained so far, show that the statistical scatter due to the intrinsic material uncertainty of shrinkage from one batch is rather small, with standard deviation of only about 7 per cent of the mean shrinkage strain. Thus, the very large uncertainty of shrinkage in design as practically experienced is due mainly to the unknown and uncertain effects of concrete composition, along with its curing history, and to the randomness of environment.
2. Among ACI, CEB–FIP, and BP Models, the last one appears the best, and is also physically better justified.
3. Although the shrinkage formula of the BP Model can be linearized, statistical prediction of long-time shrinkage based on the linearized regression plot alone does not yield the best results. The best results are obtained by a combination of non-linear least-squares optimization for determining the mean values of material parameters and a linearized regression for determining the coefficients of variation.

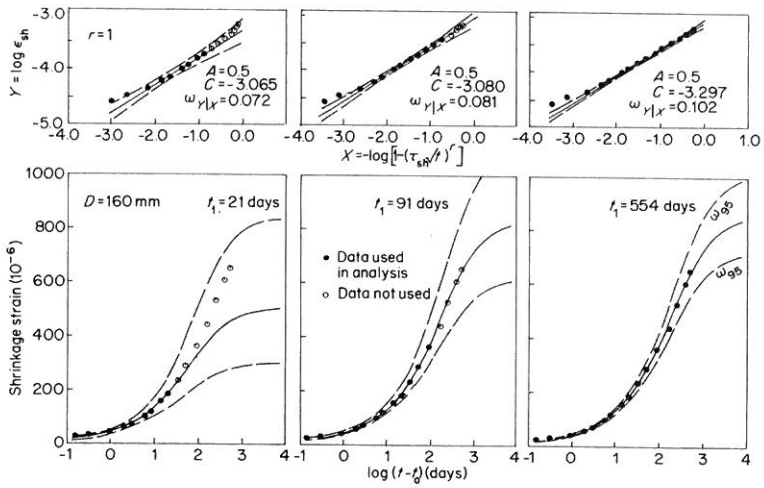

Figure 5.13 Statistics of shrinkage test data: means and 95 per cent confidence limits predicted on the basis of data measured up to time t (solid points), compared to subsequently measured data (empty points)—calculated by a combination of non-linear optimization and linear regression (Bažant *et al.*, 1985a, 1985b). Reproduced by permission of ACI

4. Specimens of reduced size may be used as a means of accelerated testing of shrinkage. Long-time shrinkage can be predicted well on the basis of three- or four-week measurements of shrinkage of cylinders with diameter 80 mm.
5. By carrying out short-time (three weeks) accelerated shrinkage tests for the given concrete to be used in a particular structure, one eliminates most of the shrinkage uncertainty due to concrete composition, which is the largest source of error. However, the statistical variation due to random environment, which is very large, must be superimposed on the long-time predictions obtained with the method proposed in this work.
6. The prediction based on minimizing the sum of squared errors in shrinkage strain is better than the prediction based on minimizing the sum of squared errors in the inverse of square of shrinkage strain. Whereas the latter prediction can be obtained by linear regression in transformed variables, the former prediction necessitates the use of non-linear optimization.

5.4.3 Bayesian statistical extrapolation of creep

A Bayesian approach for the prediction of creep was presented by Bažant and Chern (1984). The method is described briefly as follows. The 'prior' information, i.e. the coefficient of variation of deviations from the creep law for concrete is combined, according to Bayes's theorem (see, e.g. Winkler, 1972; Box and Tiao,

1973; Martz and Waller, 1982), with the probability of the creep values measured on a given concrete for a relatively short time to yield the 'posterior' probability distribution of the creep values of the given concrete for any load duration and age at loading. The linearity of creep and the normal distribution of errors are assumed for the given concrete as well as the 'prior' information. The Bayesian statistical prediction for basic creep of concrete is outlined in the following. Many creep prediction formulas may be transformed into a linearized form as follows:

$$J(t,t') = q_1 x + q_2 + e \tag{5.16}$$

where $J(t,t')$ = creep compliance, t = current time, t' = age at loading; x may be called the reduced time, q_1, q_2 are material parameters, and e is the error. In particular, for the double power law, one may set

$$q_1 = \phi_1/E_0; \qquad q_2 = 1/E_0; \qquad x = (t'^{-m} + \alpha)(t-t')^n \tag{5.17}$$

where E_0, ϕ_1, m, n, and α are the material parameters included in the double power law. Parameters m, n, and α must be considered as fixed, while parameters E_0 and ϕ_1 are random and may be expressed from the random basic material parameters q_1 and q_2. According to the Bayes theorem, the posterior probability density distribution $f''(q_1,q_2)$ is expressed by the prior probability density distribution $f'(q_1,q_2)$ as follows:

$$f''(q_1,q_2) = kP(J_j|q_i)f'(q_1,q_2) \tag{5.18}$$

$$k = \left[\int_{-\infty}^{\infty}\int_{-\infty}^{\infty} P(J_j|q_i)f'(q_1,q_2)\,dq_1\,dq_2\right]^{-1};$$

$$J_j = J(x_j) \qquad (j = 1,2,\ldots,N) \tag{5.19}$$

where $P(J_j|q_i)$ is the probability of observing values J_j under the condition that the parameter values are q_i. Also, $x_j = j$th reduced time, N = total number of reduced times. Assuming that J_j are statistically independent of each other and normal random variables for certain q_1, q_2, and x_j with the mean $q_1x_j + q_2$ and the standard deviation σ, and that σ is independent of x, the posterior probability of $J(x)$ for a given value J is obtained as follows:

$$P[J(x) < \hat{J}] = \int_{-\infty}^{\infty}\int_{-\infty}^{\infty} \phi[y(q_1,q_2)]f''(q_1,q_2)\,dq_1\,dq_2 \tag{5.20}$$

$$\phi[y(q_1,q_2)] = P[J(x) < \hat{J}|q_1,q_2] = [1/(\sigma\sqrt{2\pi})]\int_{-\infty}^{y} \exp(-z^2/2\sigma^2)\,dz;$$

$$f''(q_1,q_2) = a_0 \exp\left[-(1/2)\sum_{i=1}^{N}\{y(q_1,q_2)\}^2\right] f'(q_1,q_2);$$

$$a_0 = k(\sigma\sqrt{2\pi})^{-N}; \qquad y(q_1,q_2) = (\hat{J} - q_1x - q_2)/\sigma \tag{5.21}$$

If $f'(q_1,q_2)$ is a normal distribution, the posterior (updated) probability that the creep compliance $J(x)$ at reduced time x will be less than some given value $\hat{J}$ may be calculated by the above equations. An example of the Bayesian prediction is shown in Fig. 5.14. It is shown that this method gives good prediction of long-time creep, given the 'prior' information and short-time creep data.

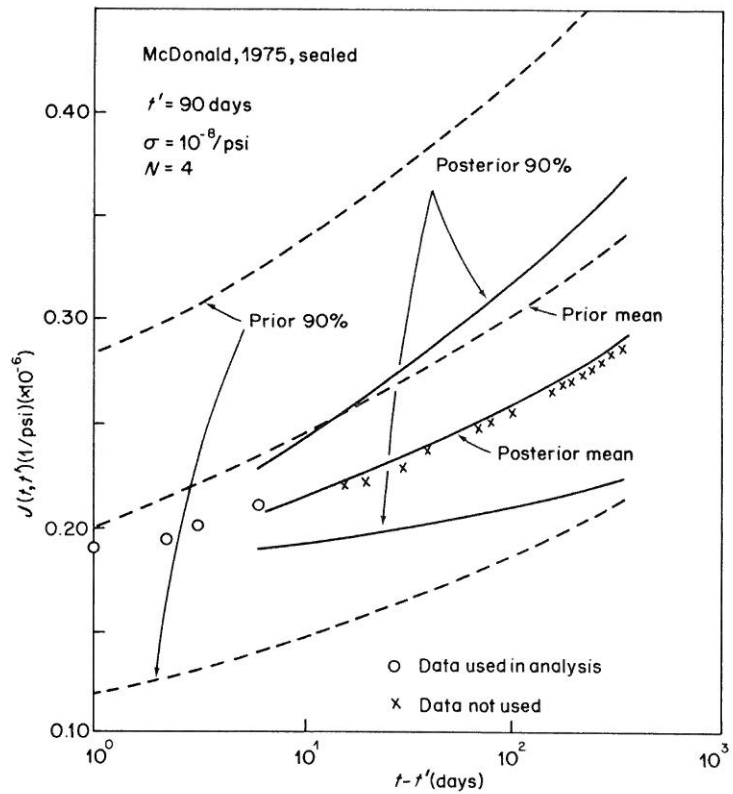

Figure 5.14 Example of Bayesian extrapolation of creep: data of McDonald (1975), assuming only the first four points to be known and the rest of them unknown (Bažant and Chern, 1984) (1 psi = 6.89 kPa). Reproduced by permission of ACI

5.4.4 Bayesian statistical extrapolation of shrinkage

Similar to the prediction of the creep of concrete, a couple of methods for Bayesian statistical extrapolation of shrinkage have been reported (Bažant *et al.*,

1985a; Tsubaki *et al.*, 1985; Bažant *et al.*, 1987). A brief summary of these studies is given in the following.

In their works, the prior statistical information available in the literature on concrete shrinkage is exploited to improve the extrapolation of short-time shrinkage measurements into long times. It is found that this approach can significantly improve the long-time predictions, as compared to the predictions obtained by statistical regression from the measured data alone, provided that the measured data do not lie at the margins of the scatter band of the prior information. If the measured data lie outside the 90 per cent confidence band of the prior information, the method fails. The method of analysis consists in Latin hypercube sampling of random parameters of the shrinkage formula for the prior information (Bažant, 1985), and in adjustments of the weights of the samples on the basis of Bayes's theorem. The shrinkage formula of the BP model, which is justified by diffusion theory, is used. This formula gives prior mean predictions which are rather close to the measured short-time data. Using this formula, good long-time predictions can be obtained even with measurements of only three-day duration. The formulas from the ACI and CEB–FIP models are found unsuitable for Bayesian extrapolation. An improvement of the formula for predicting the final shrinkage strain from concrete composition is also presented (cf. Figs. 5.15 and 5.16).

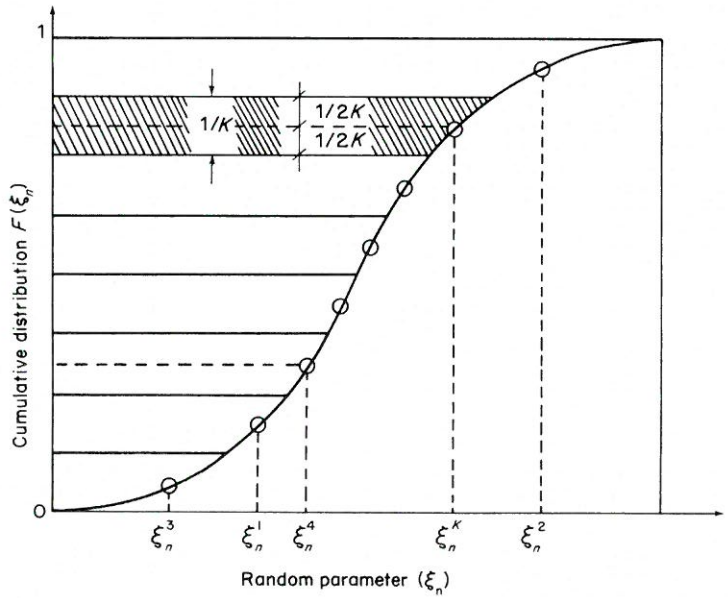

Figure 5.15 Bayesian extrapolation of shrinkage: Partitioning of range of random variable into intervals (Bažant *et al.*, 1985a). Reproduced by permission of ACI

5.4.5 Remarks

Due to internal and external factors, the existing experimental data of creep and shrinkage of concrete involve a significant amount of statistical variation. In this section, two statistical methods are introduced in order to deal with the statistical

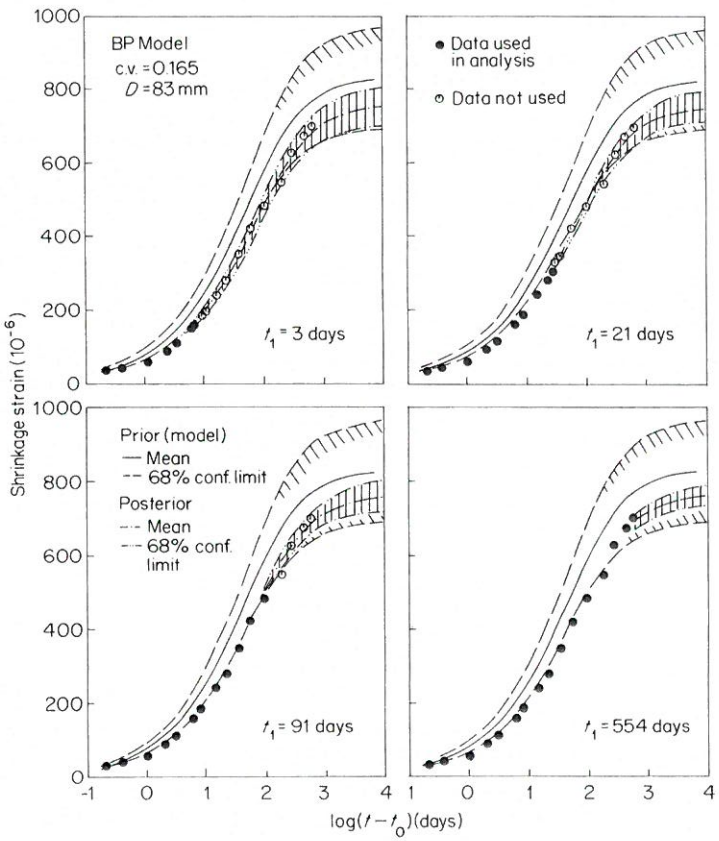

Figure 5.16 Example of Bayesian extrapolation of shrinkage: data of cylinder specimens ($D = 83$ mm) with BP model (Bažant *et al.*, 1985a). Reproduced by permission of ACI

variation of creep and shrinkage in their predictions: i.e. regression and Bayesian extrapolation. Their effectiveness depends on the choice of the deterministic models used in these schemes. It seems that more refinement of existing deterministic models is necessary, to be more suitable in the statistical schemes. Also, the recent works suggest some possibility of an accelerated measuring method to be used in the prediction of creep and shrinkage.

For the general information on statistical methods, see Raiffa and Schlaifer (1961), DeGroot (1970), Bendat and Piersol (1971), Box *et al.* (1978), and Von Mises (1981).

5.5 PROBABILISTIC ANALYSIS FOR INTERNAL UNCERTAIN FACTORS

5.5.1 Effect of stochastic nature of creep

The internal uncertainty in concrete creep is that caused by the stochastic creep process which is inherent in the microscopic creep mechanism. As the application of stochastic creep models listed in Section 5.3, various methods of predicting the long-time deflection of RC beams have been introduced by, for example, Benjamin *et al.* (1965), Zundelevich and Benjamin (1972), and Ditlevsen (1982). These works are essentially applications of the one-dimensional stochastic creep models for each fibre in the cross-section of reinforced concrete and prestressed concrete (PC) beams.

5.5.2 Analysis of a reinforced concrete beam column

For the analysis of an RC beam column, the following assumptions are employed in Ditlevsen's work (1982a): (1) the curvature of the beam axis at x and time t is given by $C(x,t)$ (Bernoulli modeling hypothesis (1)); (2) the stress field $\sigma(x,y,z,t)$ varies linearly with y and z in any cross-section (Bernoulli modeling hypothesis (2)); (3) the uncracked concrete section carries only longitudinal stresses (the effective section assumption); (4) the reinforcement force $N(x,t)$ is non-random and determined by a strain value $E[B(x,t) - hC(x,t)]$ in the reinforcement. Here, h is the distance between the centres of gravity of the effective concrete section and the reinforcement section (cf. Fig. 5.17). Then, the following integral equation is obtained, from which $N(x,t)$ may be determined if the bending moment history $M(x,t)$ is given.

$$N(x,t) = -(h^2A + I)[(E_sA_s)/(IA)]\int_{\tau=0}^{t} K(t,\tau)\,\mathrm{d}N(x,\tau) + (hE_sA_s/I)\int_{\tau=0}^{t} K(t,\tau)\,\mathrm{d}M(x,\tau) \tag{5.22}$$

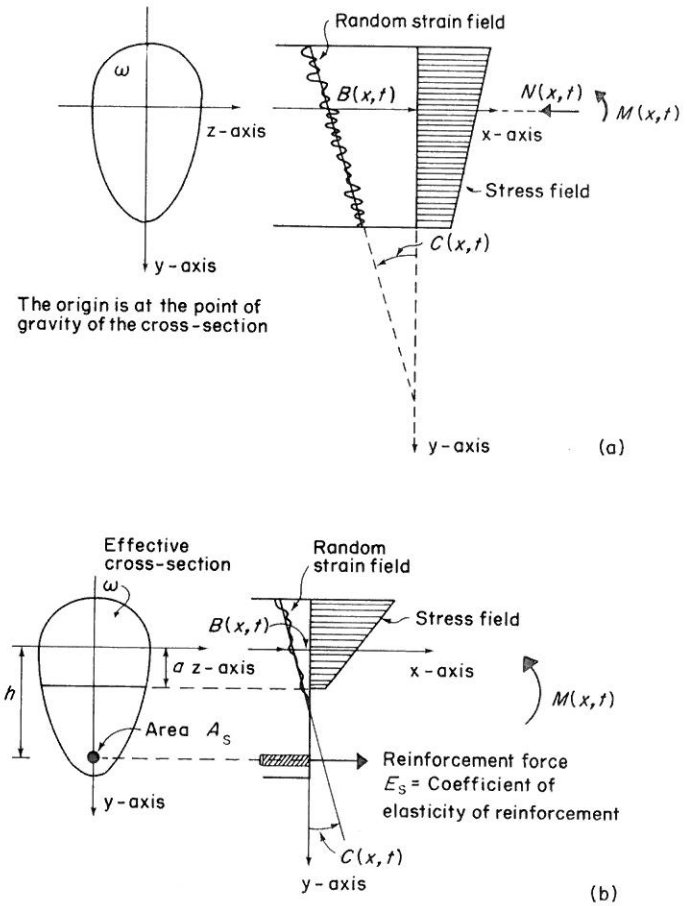

Figure 5.17 Probabilistic analysis with white noise creep model: (a) cross-section of plain concrete beam subjected to compression and bending; (b) cross-section of reinforced concrete beam subjected to bending (Ditlevsen, 1982a); (c) expectation and standard deviation of the total concrete strain for a constant externally applied normal force and for an initially applied prestressing force giving the same initial strain as the externally applied force; (d) expectation and standard deviation of the resulting normal force on the concrete section in the prestressing case and in a relaxation case of constant total strain equal to the initial strain of other cases (Ditlevsen, 1982a) (1 N = 0.102 kgf = 0.225 lbf). Reprinted with permission from O. Ditlevsen, Stochastic visco-elastic strain modeled as a second moment white noise process, *International Journal of Solids and Structures*, **18**(1), 23–5. © 1982 Pergamon Journals Ltd

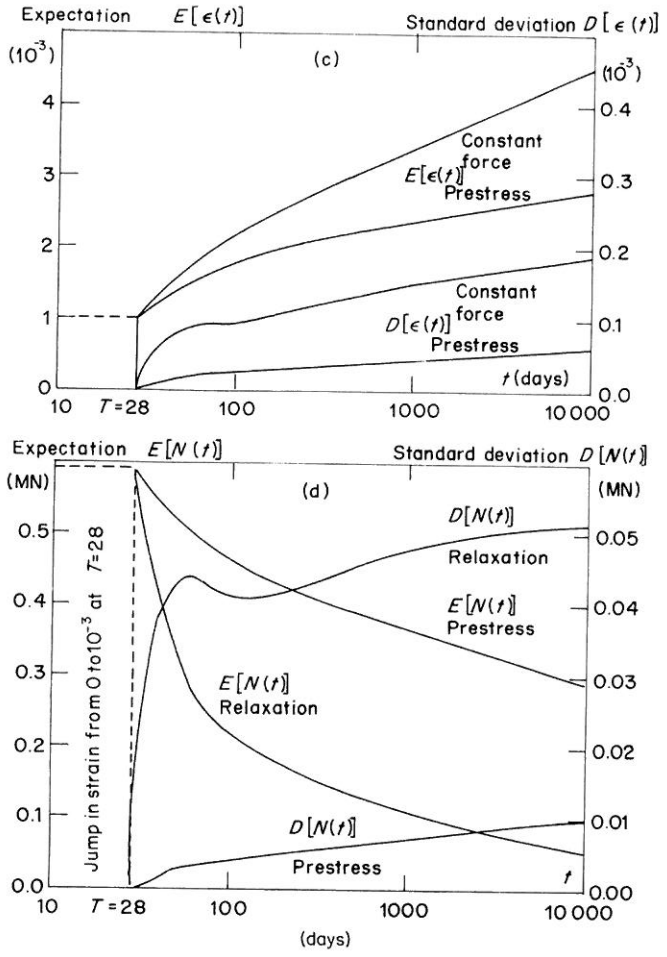

Figure 5.17 (*cont.*)

where A = area of cross-section, I = moment of inertia with respect to the z-axis, E_s = elastic modulus of reinforcement, A_s = area of reinforcement, $K(t,\tau)$ = creep function.

For a structure with an arbitrary shape, the finite element method with Monte Carlo simulation and Latin hypercube sampling may be useful. Latin hypercube

sampling, in general, needs a small number of samples relative to random sampling such as that used in the Monte Carlo method. The method is particularly efficient (in terms of a decrease in number of necessary computer runs) for establishing trends from large finite element analyses of complex structures. An example of a reliability analysis for a prestressed simply supported beam under transverse loading is shown in Anderson (1982) (cf. Fig. 5.18). The creep function is in the following form.

$$J(t,t') = (1/E_c) + [a + b(t')^n]\{1 - \exp[-(t-t')/\tau]\} \tag{5.23}$$

where $J(t,t')$ = creep compliance function, t = current time, t' = age at loading, E_c, a, b, n, τ = material constants. Here, the material property variables a, b, and n are random, together with the load variables. Then, the fibre strain at the centre of

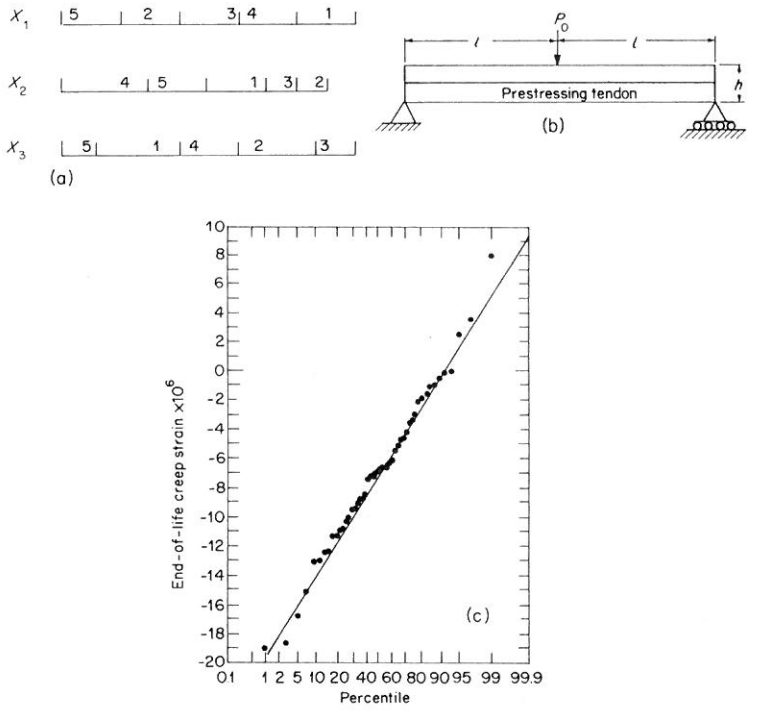

Figure 5.18 Latin hypercube sampling: (a) sampling with three random variables and five computer runs; (b) prestressed simply-supported beam under transverse loading; (c) normal probability plot for the beam fibre strain (sample size 50) (Anderson, 1982). © 1982. Reprinted by permission of John Wiley & Sons Ltd

the beam on the underside is obtained as follows:

$$\varepsilon[-(h/2),t]=[(P_0hl)/(4I)]J(t,t_0) - [\varepsilon_0 J(t,t^*)]/[(A_c/A_sE_s)+J(t,t^*)] \quad (5.24)$$

where P_0 = transverse load, h = depth of the beam, l = half length of the beam, t = current time, t_0 = age when load P_0 is applied, ε_0 = tendon initial strain at $t=t^*$, t^* = age when prestress is applied. Also, E_s = the steel modulus, I = the cross-sectional moment of inertia, and A_s and A_c = the cross-sectional steel and concrete areas respectively. Parameters a, b, and n were assumed to be uniformly distributed, while the random load variable P_0 (cf. Fig. 5.18(b)) and the age at loading t_0 are normally distributed variables.

Then, by the Latin hypercube sampling, the probability density function of the fibre strain at the base of the beam was estimated. Figure 5.18(c) illustrates the cumulative frequency distribution of the results plotted on normal probability paper, from which the mean and the standard deviation are obtained.

5.5.3 Sampling methods and other remarks

In this section, some examples for the application of the one-dimensional stochastic creep models to concrete beams are introduced. If the stochastic model has a simple form, then the mean and the standard deviation can be obtained in a simple manner. Otherwise, it is necessary to use some numerical procedure such as the Monte Carlo method.

The method of sampling becomes important for computational efficiency. Some works suggest the Latin hypercube sampling to be efficient. Details of the Latin hypercube sampling procedure are found in MaKay *et al.* (1976). See also Bažant (1985), Bažant and Liu (1985), and Křístek and Bažant (1985).

The Latin hypercube sampling applications to creep and shrinkage have originally been made under the assumption that the material parameters are statistically independent. In reality, many of the parameters of creep and shrinkage models are correlated, e.g. the strength and the water–cement ratio. A method to handle such correlations has been developed by Xi and Bažant (1987). They analysed existing data and used the method of maximum likelihood to establish the joint multivariate probability distribution of the random parameters of the BP model. They tested the hypothesis of mutual dependence among the parameters on the basis of the χ^2-distribution. To extend the Latin hypercube sampling to the case of correlated multinormal random parameters, they transformed the random parameters of the BP model to new random parameters which represent linear combinations of the original parameters. The transformation is orthogonal, with a transformation matrix consisting of the eigenvectors of the inverse of the covariance matrix. The fact that the transformed random parameters are uncorrelated makes it possible to obtain equal probability samples for the Latin hypercube sampling. These samples are then projected by

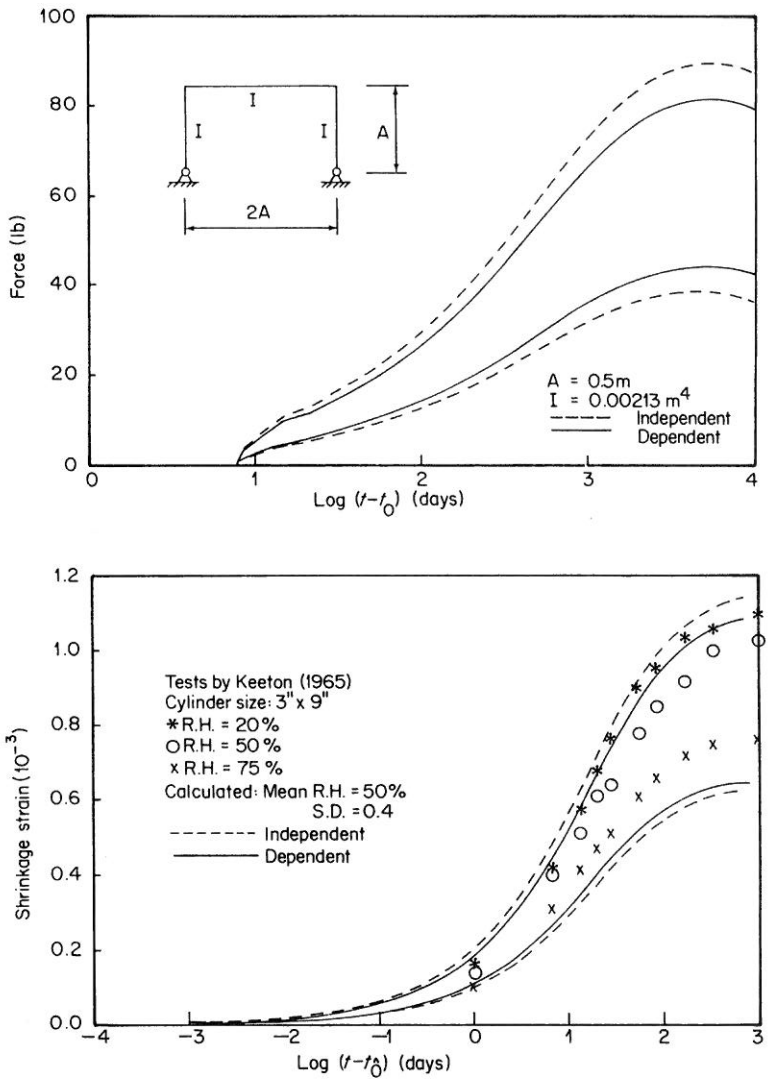

Figure 5.19 Effect of statistical correlation among the random parameters of the BP model on the response curves of mean ± standard deviation for a shrinkage specimen and a two-hinge frame (after Xi and Bažant, 1987)

an inverse transformation to obtain equal probability samples of the original random parameters. Numerical examples confirmed practical feasibility and a good agreement with the scatter observed in some previous experiments (Fig. 5.19). Generally, the existance of correlation reduces the width of the scatter band of mean $\pm$ standard deviation. Thus, the neglect of correlation is on the safe side.

5.6 PROBABILISTIC ANALYSIS FOR EXTERNAL UNCERTAIN FACTORS

5.6.1 Effect of stochastic environmental conditions

The effect of variation of environmental conditions on concrete structures is, in most cases, larger than that of the variation of internal factors such as material properties and mix proportions (Russell *et al.*, 1982).

Recently, the data on the static behaviour of PC bridges has been reported (Jávor, 1985). According to that report, the creep and shrinkage deformations generally settle after seven years and, in the next period, due to the temperature changes of the atmosphere, oscillations of 1–1.5 cm for the PC bridges with the span 60–80 m are observed, depending on the quality of concrete. This fact implies that the influence of the environmental conditions on both RC and PC structures is significant.

Since the behaviour of concrete structures in service has a primary importance for the judgement of their safety and serviceability, it is necessary to continue to observe their behaviour in order to obtain some data on the real behaviour and the state of stress of structures. At the same time, it would be desirable from the engineering point of view to predict the long-term behaviour of concrete structures subjected to various environmental conditions. In this section, some analytical methods, together with their applications, for this purpose are introduced.

5.6.2 Spectral analysis methods

The effect of random temperature change on general structures was discussed by, for example, Heller (1976a, 1976b, 1979), in which the temperature variation is modeled by a sum of a narrow band process accounting for yearly variations and another process representing daily variations. Tsubaki and Bažant (1982) investigated the effect of random change of ambient humidity on the shrinkage and stresses of a viscoelastic concrete hollow cylinder. Bažant (1982b) used a different method to solve the above problem. In his work, a modified Wiener–Khintchine relation obtained by shifting the time scale was used (cf. Fig. 5.20), instead of the impulse response function method used in Tsubaki and Bažant (1982), in order to take into account the non-linearity in time (i.e. non-

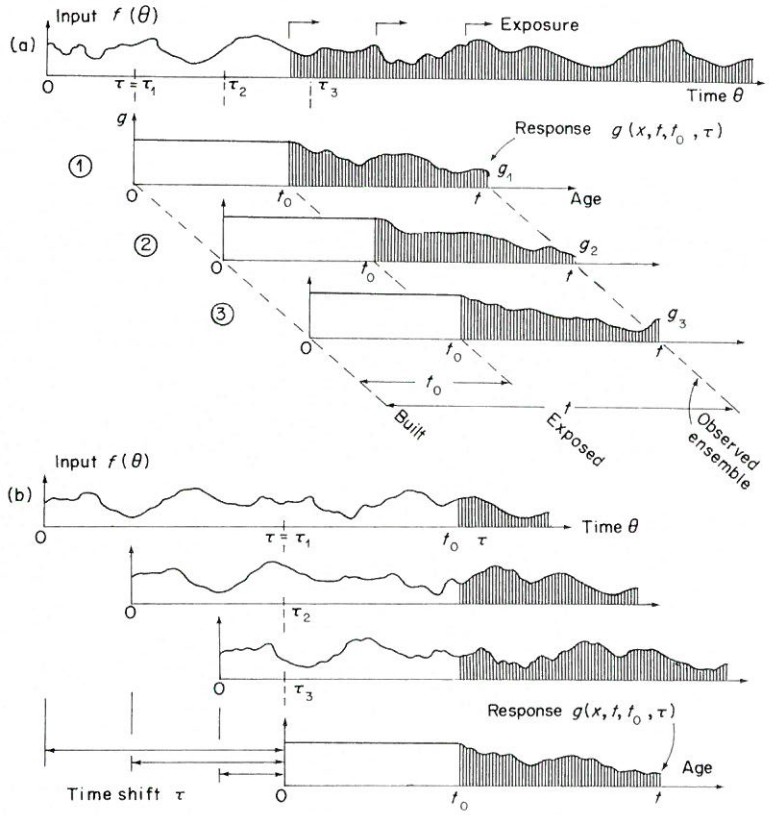

Figure 5.20 The aging aspect of response of a concrete structure to random environment; (a) example of response realization; (b) shift of birth time, (Bažant, 1986). Reproduced by permission of ASCE

stationarity) due to aging of concrete. This method is more efficient in calculation than the method using an impulse response function. With this method, the relationship between the power spectral density S_f of input f and the power spectral density S_g of response g can be expressed as follows:

$$S_g(\omega, x, t, t_0) = |Y(\omega, x, t, t_0)|^2 S_g(\omega) \tag{5.25}$$

where ω, x, t, t_0 are the circular frequency of the input, the spatial coordinates, the age of concrete, and the age of the concrete at the time when the concrete was exposed to the random stationary input, respectively; Y is the frequency response

function of the system. The above equation is the same as the classical result for stationary response of non-aging systems, except for the presence of arguments t and t_0. On the other hand, the relationship between the autocorrelation functions of the input, R_f, and the output, R_g, is expressed as follows, if the impulse response function is used:

$$R_g(\lambda, x, t, t_0) = \int_{-\infty}^{\infty}\int_{-\infty}^{\infty} R_f(\xi - \eta + \lambda) y(x, t, t_0, \xi) y(x, t, t_0, \eta)\, \mathrm{d}\xi\, \mathrm{d}\eta \qquad (5.26)$$

$$R_f(\lambda) = \lim_{T\to\infty} [1/(2T)] \int_{-T}^{T} f(\theta) f(\theta + \lambda)\, \mathrm{d}\theta;$$

$$y(x, t, t_0, \xi) = [1/(2\pi)] \int_{-\infty}^{\infty} Y(\omega, x, t_0 + \xi, t_0) \mathrm{e}^{i\omega\xi}\, \mathrm{d}\omega \qquad (5.27)$$

where y is called the impulse response function of the system and θ is the time. Also, λ = time, f = input, $i = \sqrt{-1}$. Note that Eq. (5.25) is algebraic, while Eq. (5.26) is given by a double integral. From a computational point of view, Eq. (5.25) is more convenient for the spectral analysis of aging systems.

The detail of the above method for aging linear systems exposed from a certain age, t_0, to ergodic random input is given in the following (cf. Bažant, 1986).

The principal idea is that the response, while non-stationary with respect to time and age, is stationary and ergodic with regard to the birth time (the time when the system was built). Consequently, the instantaneous statistical characteristics of all possible response realizations at a chosen age, t, may be determined as the characteristics of the response at age t (and at a fixed exposure age, t_0) as the birth time is varied, i.e. as the input history is shifted in time against the instant when the system was built (cf. Fig. 5.19). By this idea the spectral method is generalized for aging systems, using a frequency response function and a spectral density of response that depend on both the current age t and the age t_0 when the exposure begins.

In summary, the following conditions are obtained:

1. The statistical characteristics of the response of an ageing linear system subjected to ergodic random input may be determined by considering a fixed age of the system and a fixed age at the start of exposure, and assuming that the birth time is to be varied, i.e. the input to be shifted in time against the instant when the system is built. The response, while non-stationary in time, becomes then a stationary ergodic random process as function of the birth time; and response averaging over the birth time becomes equivalent to instantaneous ensemble averaging over all possible realizations.
2. The spectral method can be generalized for aging linear systems under ergodic input. The relationship between the spectral densities of input and response is algebraic, as shown in Eq. (5.25), similar to the case of stationary response, although the frequency response function needs to be obtained by solving integral or differential (rather than algebraic) equations in time.

3. In the special case of non-stationary response of non-aging systems under ergodic input, this formulation appears to offer a simpler alternative to the existing formulations, taking advantage of ergodicity with respect to the birth time.

The above method is used to solve the problem of an aging half-space exposed to oscillating humidity (Bažant and Wang, 1984) (cf. Fig. 5.21).

5.6.3 Spectral analysis by the finite element method

In order to deal with a concrete structure with an arbitrary geometry, it is necessary to use some numerical method. In the following, a spectral analysis scheme using the finite element method is summarized, with an emphasis on the environmental temperature change.

The frequency response function for a stationary heat conduction problem can be obtained from the following matrix equation for temperature $\boldsymbol{\theta}$ and flux $\mathbf{q}$.

$$[\kappa \mathbf{K}_2 + i\omega \mathbf{K}_1]\boldsymbol{\theta} = \mathbf{q} \qquad (5.28)$$

$$\mathbf{K}_1 = \sum_{\mathrm{el}} \int_v \boldsymbol{N}^T \mathbf{N}\, \mathrm{d}V; \qquad \mathbf{K}_2 = \sum_{\mathrm{el}} \int_v \boldsymbol{N}_{,i}^T \mathbf{N}_{,i}\, \mathrm{d}V \qquad (5.29)$$

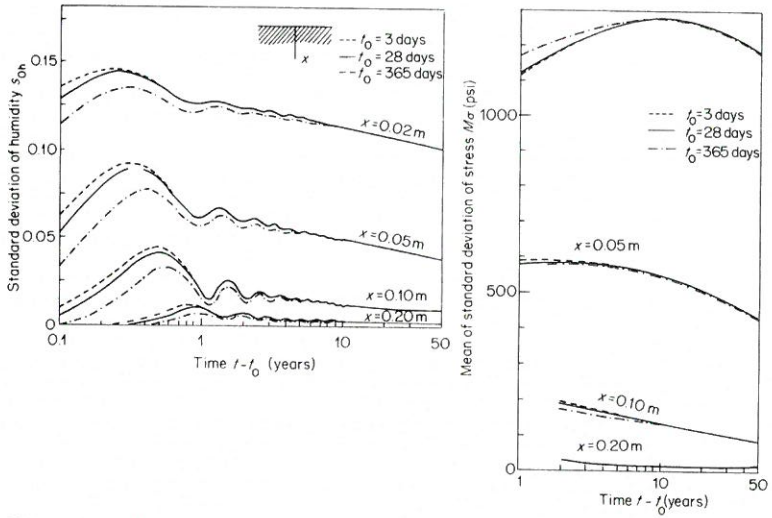

Figure 5.21 Spectral method for an aging half-space exposed at surface to humidity oscillating with a period of one year (Bažant and Wang, 1984a) (1 m = 3.28 ft). Reproduced by permission of ASCE

where $i = \sqrt{-1}$, κ = thermal diffusivity, ω = circular frequency of the input, and $\mathbf{N}$ = interpolation function. Also, V = volume of the domain, $N_{,i} = \partial \mathbf{N}/\partial x_i$, $x_i = i$th component of coordinates. Then, the frequency response functions of stresses $\boldsymbol{\sigma}$ are obtained, solving the following matrix equation for displacement $\mathbf{u}$:

$$\mathbf{K}\mathbf{u} = \mathbf{F}'' \tag{5.30}$$

$$\mathbf{K} = \sum_{el} \int_v \mathbf{B}^T \mathbf{D} \mathbf{B}\, dV; \qquad \mathbf{F}'' = \sum_{el} \int_v \mathbf{B}^T \mathbf{D} \boldsymbol{\varepsilon}''\, dV;$$

$$\boldsymbol{\sigma} = \mathbf{D}(\boldsymbol{\varepsilon} - \boldsymbol{\varepsilon}''); \qquad \boldsymbol{\varepsilon} = \mathbf{B}\mathbf{u} \tag{5.31}$$

where $\mathbf{D}$ is the tangential modulus matrix, $\boldsymbol{\varepsilon}$ is the total strain, and $\boldsymbol{\varepsilon}''$ is the strain vector due to thermal expansion. For a stationary problem, $\mathbf{D}$ is obtained by replacing the Young's modulus by the complex modulus calculated from the relaxation modulus E_R. The application of this method is shown by Bažant and Wang (1984a, b, c) (cf. Figs 5.22–24). On the analysis method using finite elements for structures in which mechanical material properties such as stiffness exhibit one-dimensional spatial random variation, see Vanmarcke and Grigoriu (1983). It is reported that this method efficiently evaluates the first- and second-order statistics of the deflection of a beam whose rigidity varies randomly along its axis. The stationary random variation is characterized by three parameters: the mean, the standard deviation, and the scale of fluctuation. For the extension of this method to two- and three-dimensional structures, see Vanmarcke (1983).

5.6.4 Spectral analysis by the boundary element method

The boundary integral method, or the boundary element method (BEM), can also be applied to creep and shrinkage analysis of concrete structures such as an analysis of a massive concrete structure subjected to a stationary random periodic temperature change. Since the BEM needs less elements, in general, than the finite element method (FEM), it is particularly effective for a three-dimensional concrete structure. The problem dealt with in the previous section by the FEM can also be solved using the BEM. For a stationary two-dimensional heat conduction problem, the frequency response function of temperature θ is obtained by the following integral equation (cf. Fig. 5.25):

$$c(\mathbf{y})\theta(y) + \int_s q^*(\mathbf{y}, \mathbf{y}_1)\theta(\mathbf{y}_1)\, dS(\mathbf{y}_1)$$

$$= \int_s \theta^*(\mathbf{y}, \mathbf{y}_1) q(\mathbf{y}_1)\, dS(\mathbf{y}_1) \tag{5.32}$$

$$q^*(\mathbf{y}, \mathbf{y}_1) = \partial\theta^*(\mathbf{y}, \mathbf{y}_1)/\partial n; \qquad \theta^*(\mathbf{y}, \mathbf{y}_1) = [1/(4i)]H_0^{(2)}(\beta r);$$

$$\beta = (i-1)\sqrt{[(\rho c \omega)/(2K)]}; \qquad r = |\mathbf{y} - \mathbf{y}_1|;$$

$$q(\mathbf{y}_1) = \partial\theta(\mathbf{y}_1)/\partial n; \qquad c(\mathbf{y}) = \tfrac{1}{2} \tag{5.33}$$

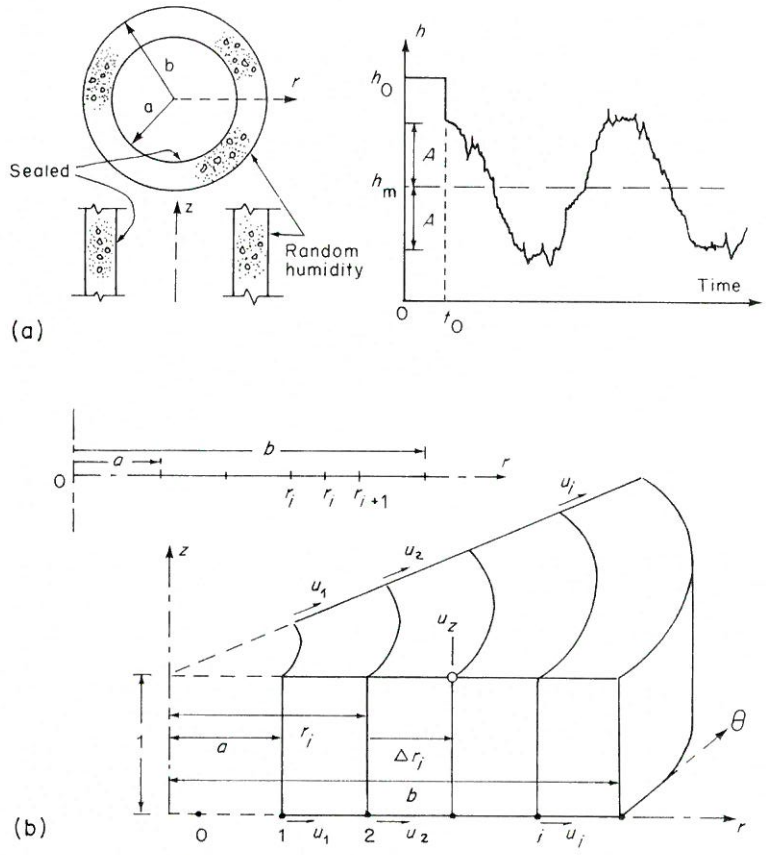

Figure 5.22 Spectral method with the finite element method: (a) a cylindrical vessel and random variation of surface humidity h; (b) one-dimensional discretization of the cylindrical wall (Bažant and Wang, 1984c). Reproduced by permission of ASCE

where $i = \sqrt{-1}$, $\omega = 2\pi/T$, and T is the period of a temperature change. Also, K, ρ, and c, respectively, stand for the heat conductivity, the density, and the specific heat of the structural material; $H_n^{(2)}$ is the nth-order Hankel function of the second kind; $\partial/\partial n$ is the directional derivative in the direction of the outer normal $\mathbf{n}$ on the boundary surface S; $\mathbf{y}$ = field point, $\mathbf{y}_1$ = source point, S = boundary surface of the domain, q = flux.

Then, the frequency response functions of the stresses are obtained by the

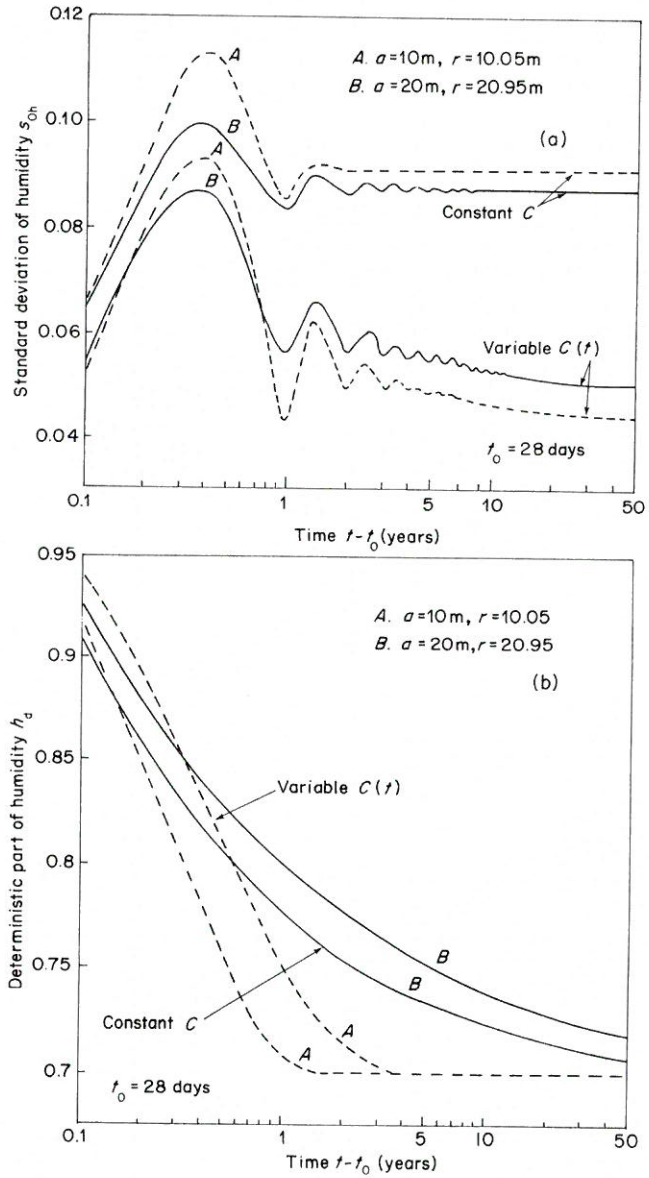

Figure 5.23 Example of the spectral method with the finite element method: time evolution of pore humidity at 5 cm below exposed surface: (a) standard deviation; (b) deterministic part (Bažant and Wang, 1984c) (1 m = 3.28 ft). Reproduced by permission of ASCE

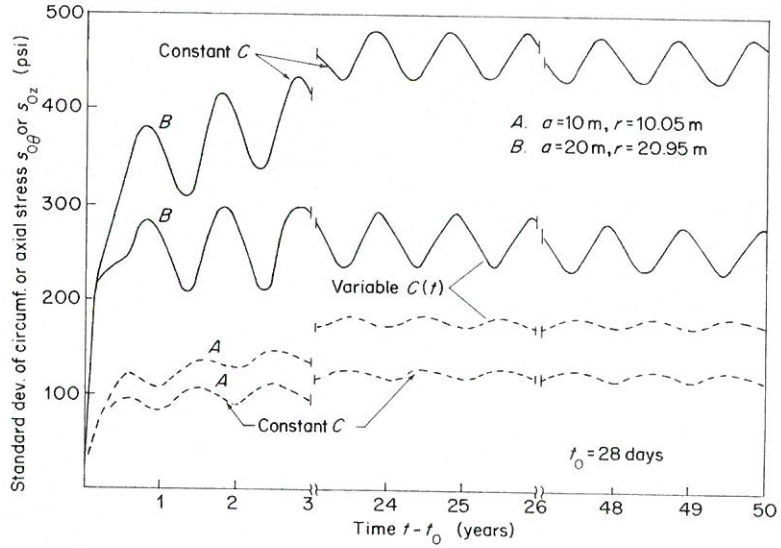

Figure 5.24 Example of the spectral method with the FEM: time evolution of standard deviation of circumferential or axial shrinkage stresses, the mean of standard deviation, and its amplitude (Bažant and Wang, 1984c) (1 psi = 6.89 kPa, 1 m = 3.28 ft)

following integral equation for displacement u_i and traction f_i:

$$C_{ki}(\mathbf{y})u_i(\mathbf{y}) + \int_s f^*_{ki}(\mathbf{y}, \mathbf{y}_1)u_i(\mathbf{y}_1)\,\mathrm{d}S(\mathbf{y}_1) = \int_s u^*_{ki}(\mathbf{y}, \mathbf{y}_1)f_i(\mathbf{y}_1)\,\mathrm{d}S(\mathbf{y}_1) + b_k(\mathbf{y}) \tag{5.34}$$

$$C_{ki}(\mathbf{y}) = (\tfrac{1}{2})\delta_{ki} \tag{5.35}$$

where u^*_{ki} is the fundamental solution of the two-dimensional isotropic elastic body, and f^*_{ki} is the traction component corresponding to u^*_{ki}; b_k is the body force term due to the temperature distribution $\theta(\mathbf{x})$, and δ_{ki} is the Kronecker delta. Also, $u_i = i$th component of displacement vector, and $f_i = i$th component of surface traction vector.

The details of the analysis method is shown in Tsubaki (1984a, b), for example. An example of an analysis using the above analysis method is shown in Figs 5.26, 5.27 and Table 5.2. Figures 5.26 and 5.27 show the distributions of the temperature and stresses of a concrete structure subjected to a periodic temperature change. The length and slope of a line segment in these figures stand for the

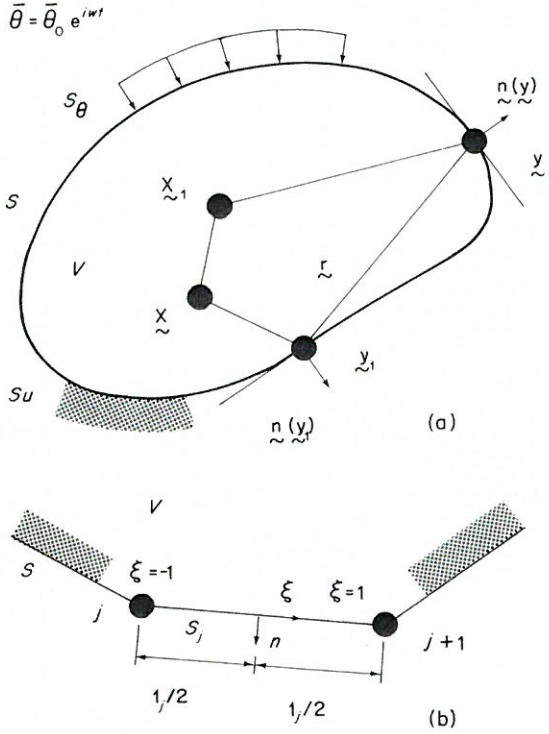

Figure 5.25 Spectral method with the BEM: (a) domain and boundary subject to a periodic input; (b) linear boundary element (Tsubaki, 1984b). Reproduced by permission of JCI

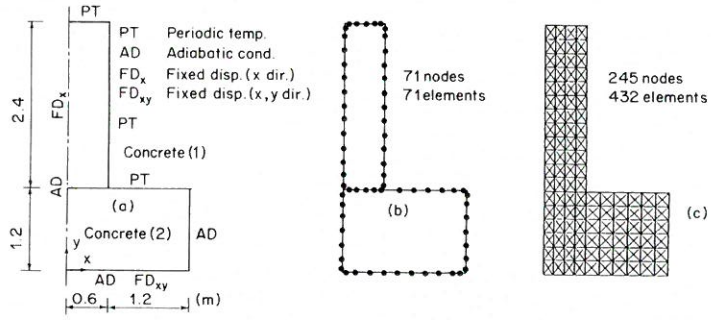

Figure 5.26 Example of the spectral method with the BEM: (a) massive concrete structure subjected to a periodic temperature input—boundary conditions (b) boundary element discretization (c) finite element discretization (Tsubaki, 1984b) (1 m = 3.28 ft). Reproduced by permission of JCI

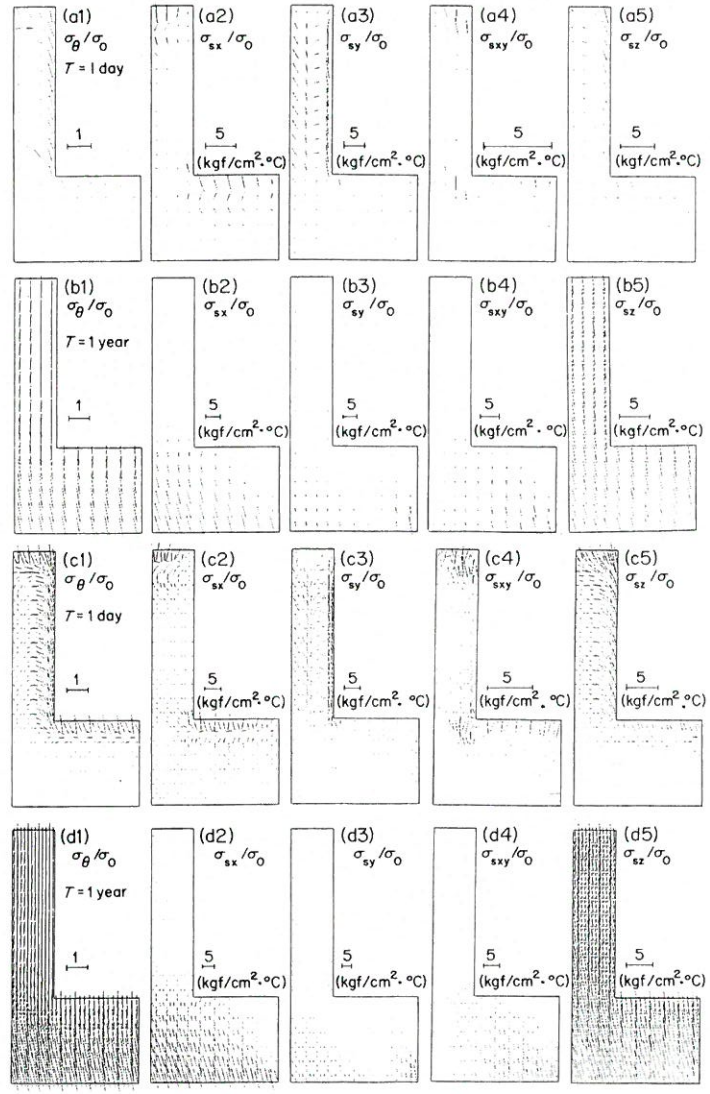

Figure 5.27 Example of the spectral method with the BEM: (a, b) distribution of temperature and stresses by the BEM (Tsubaki, 1984b) (1 kgf/cm^2 = 98.1 kPa = 14.2 psi); (c, d) distribution of temperature and stresses by the FEM (Tsubaki, 1984b) (1 kgf/cm^2 = 98.1 kPa = 14.2 psi)

Table 5.2 Example of the spectral method with the Boundary Element Method: material constants (a) and complex modulus (b) of concrete (Tsubaki, 1984b) 1 kgf/cm^2 = 98.1 KPa = 14.2 psi.

(a)	Material constants	Concrete (1)	Concrete (2)
Heat cond.	K (kcal/m·day·°C)	57.6	45.6
Density	ρ (kg/m^3)	2300	2400
Spec. heat	c (kcal/kg·°C)	0.24	0.27
Therm. diff.	κ (m^2/day)	1.044×10^{-1}	7.037×10^{-2}
Age	τ (days)	1825	3650
Poisson ratio	ν	0.17	0.17
Exp. coeff.	α (°C^{-1})	10×10^{-6}	10×10^{-6}

(b)	Complex modulus	E	Concrete (1)	Concrete (2)
$T = 1$ day	Re(E)	(kgf/cm^2)	2.158×10^5	2.191×10^5
	Im(E)	(kgf/cm^2)	2.221×10^3	1.317×10^3
$T = 1$ year	Re(E)	(kgf/cm^2)	1.570×10^4	1.233×10^4
	Im(E)	(kgf/cm^2)	1.570×10^4	1.233×10^4

magnitude and the phase angle of the temperature and stresses respectively. It is observed that the result obtained by BEM is in good agreement with that by FEM.

5.6.5 Analysis method for model uncertainty

H. Madsen and Bažant (1983) also reported the effects of variations in environmental humidity and temperature, together with those of variations in shape and size of the structure and other parameters related to mix composition and strength, on concrete structures (cf. Table 5.3). The effects of variations of these parameters at different points of the same concrete structure on the total uncertainty were investigated. The model uncertainties related to choosing one specific set of shrinkage and creep formulas were also discussed. Model uncertainty was accounted for by applying a random factor or a model uncertainty factor to each term: shrinkage, basic creep, and drying creep. Although any deterministic creep and shrinkage formula can serve as the basis for this approach, the BP formulas are chosen in their work. The formula for shrinkage is then:

$$\varepsilon_{sh}(t, t_0) = \psi_1 \varepsilon_{sh\infty} k_h S(t, t_0) \tag{5.36}$$

Also, the formula for creep is

$$J(t, t') = \psi_2[(1/E_0) + C_0(t, t')] + \psi_3[C_d(t, t', t_0) - C_p(t, t', t_0)] \tag{5.37}$$

where $\varepsilon_{sh}(t, t_0)$ = shrinkage strain, t = current time, t_0 = age of concrete when

Table 5.3 Analysis method for model uncertainty: example of influence parameters (Madsen and Bažant, 1983). (1 mm = 0.0394 in, 1 kg/m^3 = 9.81 N/m^3 = 0.0625 lg/ft^3, 1 MPa = 145 psi = 10.2 kgf/cm^2).

	Parameter	Unit	Mean	Coefficient of variation
h	mean relative humidity of environment	—	0.65	0.2
h_0	initial relative humidity at which the specimen use in moisture equilibrium before time t_0	—	1.0	~0
T	mean environmental temperature	°C	20	0.1
D	effective thickness of specimen (2 × area/perimeter of cross-section)	mm	100	~0
k_s	shape factor for specimen	—	1.15	0.05
c	cement content	kg/m^3	275	0.1
w/c	water–cement ratio (by weight)	—	0.56	0.1
s/c	sand–cement ratio (by weight)	—	3.08	0.1
g/c	gravel–cement ratio (by weight)	—	4.00	0.1
a_1	parameter depending on cement type	—	1	0
f_c	28-day cylinder strength	MPa	30	0.1
t_0	age when drying begins	days	10	0

drying begins, $\varepsilon_{sh\infty}$ = ultimate shrinkage; ψ_i is the ith model uncertainty factor. Also $J(t, t')$ = creep compliance (creep function) = strain at age t caused by a uniaxial unit stress acting since concrete age t'; E_0 = asymptotic modulus ($\simeq 1.5\, E_c$ where E_c = conventional elastic modulus of concrete); C_0, C_d, C_p = functions describing the basic creep (creep at constant temperature and humidity), the increase of creep during drying, and the decrease of creep after drying;

$$C_0(t, t') = (\phi_1/E_0)(t'^{-m} + \alpha)(t - t')^n$$

(double power law) where ϕ_i, m, n, and α = parameters depending on the type of concrete; C_d = function similar to S; C_p = function similar to C_0; k_h = function of relative humidity h, defined as $(1 - h^3)$ if $h \leqslant 0.98$ or else -0.2; and S = empirical function of the variable $(t - t_0)/\tau_{sh}$, where τ_{sh} = shrinkage-square half-time proportional to the square of the dimension of the cross-section, $S(t, t_0) = [1 + \tau_{sh}/(t - t_0)]^{-1/2}$, where τ_{sh} = const. $x(k_s D)^2$, $D = 2 \times$ volume-to-surface ratio, and k_s = factor taking into account the shape of the cross-section. For $\psi_1 = \psi_2 = \psi_3 = 1$, Eqs (5.36) and (5.37) yield the ordinary BP formulas. From the test data, the mean values and coefficients of variation of the ψ-factors can be determined. The following values are used in the example:

$$\begin{array}{lll} \text{Shrinkage} & E[\psi_1] = 1; & V_{\psi_1} = 0.14 \\ \text{Basic creep} & E[\psi_2] = 1; & V_{\psi_2} = 0.23 \\ \text{Drying creep} & E[\psi_3] = 1; & V_{\psi_3} = 0.13 \end{array} \tag{5.38}$$

where $E[\psi_i]$ = mean value of ψ_i, and V_{ψ_i} = coefficient of variation of ψ_i.

Then, calculation of the response of concrete structures with the above random

creep and shrinkage properties is carried out by using the matrix formulation which allows a convenient algebraic treatment of linearly viscoelastic structures. For the computation of the statistics of the structural response, the method of point estimates for probability moments is used (cf. Rosenblueth, 1975). In the simplest form of this approach, only two points $\mu \pm s$ need to be considered for each random variable (μ = mean value of the variable, and s = standard deviation) (cf. Fig. 5.28). For the model uncertainty, see also Diamantidis (1984).

The spectral analysis of structural response is considered to be sophisticated for regular design applications. The Bayesian approach to creep prediction is also intended for special structures and would not be used in regular design. In this

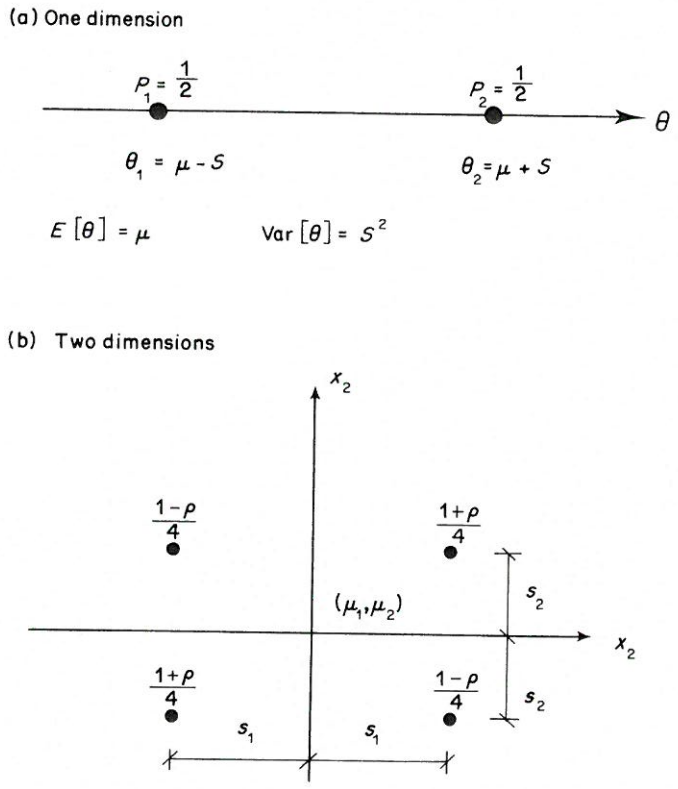

Figure 5.28 Analysis method for model uncertainty: point estimate—weights and points (Madsen and Bažant, 1983). Reproduced by permission of ACI

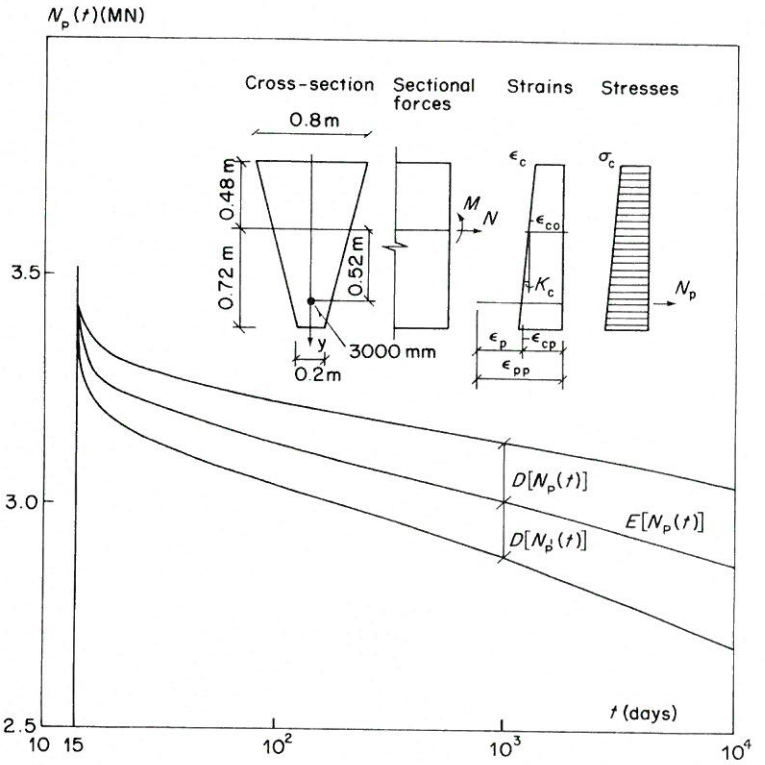

Figure 5.29 Example of model uncertainty analysis: prestress loss in prestressed beam (Madsen and Bažant, 1983) (1 N = 0.102 kgf = 0.225 lbf, 1 m = 3.28 ft, 1 mm^2 = 0.00155 in^2). Reproduced by permission of ACI

sense, the use of model uncertainty factors is a relatively simple method for an analysis of creep-sensitive structures (cf. Fig. 5.28).

This approach is considerably more efficient numerically, and therefore preferable for practical applications. In Bažant and Liu (1985), it was further proposed to introduce additional uncertainty factors, ψ_4 and ψ_5 (or zero means) which describe the uncertainty of the principle of superposition, especially the fact that for variable stress $\sigma(t)$ the error in the calculation of strain is larger than it is for constant σ. The stress–strain relationship is then written as (see Bažant and Liu, 1985)

$$\varepsilon(t) = \sigma(t_0)/E(t_0) + \int_{t_0^+}^{t} [\psi_4/E(t') + \psi_5 C(t,t')]\, d\sigma(t') \qquad (5.38a)$$

where t_0 = instant of the first loading, $C(t,t') = J(t,t') - 1/E(t')$. Equation (5.38a) is equivalent to replacing the compliance function $J(t,t')$ with the following function:

$$J^*(t,t') = J(t,t_0) + \psi_4[1/E(t') - 1/E(t_0)] + \psi_5[C(t,t') - C(t,t_0)] \quad (5.38b)$$

where $J(t,t_0)$ contains all the remaining random influence as previously described.

For the response of a system to random input, Crandall and Mark (1963), Papoulis (1965), Davenport (1972), Corotis and Vanmarcke (1975), and Newland (1975) may be consulted.

5.6.6 Analysis of precast segmental bridges

Long-term deformations and related stress redistributions in large precast segmental concrete bridges have been analysed by Buyukozturk and Wium (1984) and Wium and Buyukozturk (1984), using the FEM and taking into account the material properties and on their variability within the structure and within a given time period. The method used in their analysis simplifies the variability analysis of complex structures by reducing the number of computer runs, although it provides answers which can be used directly in the design of concrete structures. The following is the outline of the analysis method (cf. Buyukozturk and Wium, 1984). Creep is represented by a Dirichlet expansion (Bažant and Wu, 1973, Anderson, 1982), and shrinkage by a square root function of time (Bažant and Panula, 1980).

As an example, one half of a single span of multiple-span bridge is analysed, and for simplification it is assumed that the bridge is long enough so that sections at the supports and at the midspan positions do not rotate under dead loads (cf. Fig. 5.30(a)). To reduce the number of variables, it is assumed that the deformation of concrete can be represented by three variables, i.e. the stiffness, creep, and shrinkage of the concrete. The creep factor is defined in such a way that it is independent of the stiffness, but the creep and shrinkage variables are correlated.

Considering the variability of material properties, in their study, eigtheen analysis were performed on the same structure. Each material property was given seven different values. Selected combinations of these variables were used in the analyses to determine the effect of each variable on the shortening of the bridge. If α is the predicted material property, and σ_α its standard deviation, then the seven values ranged from $\alpha - 3\sigma_\alpha$ to $\alpha + 3\sigma_\alpha$. The results of the first nine analyses, for which the properties were within one standard deviation from their predicted (mean) values, are shown in Fig. 5.30(b).

The above series of analyses gives the spread in the predicted response. The next step is to fit a numerical model to the response at each time step. The eighteen

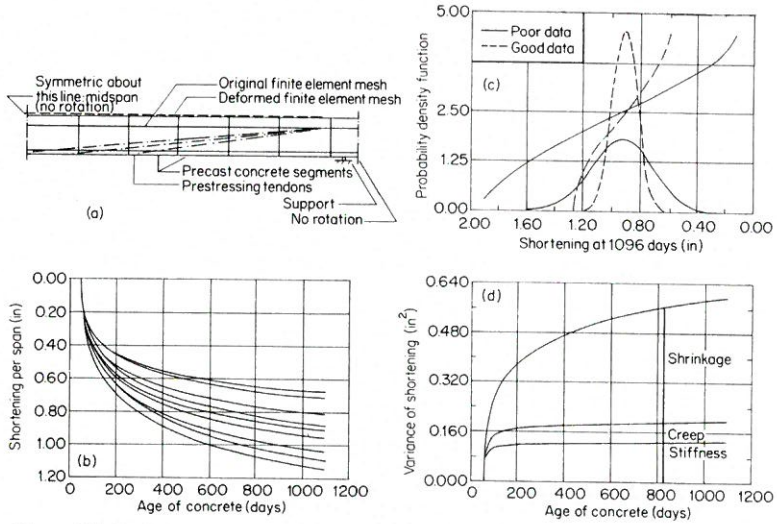

Figure 5.30 Performance evaluation of precast segmental bridges for long-term effects: (a) finite element model of bridge; (b) predicted shortening for nine different material properties (Buyukozturk and Wium 1984) (1 in = 25.4 mm); (c) distribution of shortening; (d) decomposition of variance (Buyukozturk and Wium, 1984) (1 in^2 = 645 mm^2). Reproduced by permission of ASCE

data points from the finite element analysis are used at each time step, and a polynomial is fitted to this with the linear least-squares method. The independent variables in this fitting procedure are the three material variables which represent the stiffness (x_1), creep (x_2) and shrinkage (x_3). A second-order polynomial is first used with cross terms between each two variables:

$$y = a_0 + a_1x_1 + a_2x_1^2 + a_3x_2 + a_4x_2^2 + a_5x_3 + a_6x_3^2 + a_7x_1x_2 + a_8x_1x_3 + a_9x_2x_3 \quad (5.39)$$

where y = function to be fitted.

In a well-fitted model all the coefficients (a_i) should be different from zero. This is tested with the t-statistics, which should be statistically significant (Montgomery and Peck, 1982). The complete model is first fitted to the data, and the t-statistic for each coefficient is then calculated. If the least significant coefficient is not significant, the corresponding variable is excluded from the fitting procedure for that time step, and the new model is fitted to the data. This is repeated until all the coefficients are statistically significant. This procedure is then repeated for all the time steps in the analysis. The distributions of the response at a number of time steps are then calculated with simulation. This is done in the following manner. It is assumed that the input variables are normally distri-

buted. Each input variable is discretized, and varied through the full range of probable values. The distribution of the response at a concrete age of three years is shown in Fig. 5.30(c). The distribution is also calculated for the case when the standard deviations of the material properties are reduced by testing the concrete, which is also presented in Fig. 5.30(c).

The mean, standard deviations, and certain confidence intervals for the response, can easily be calculated with this probability density function. The cumulative distribution function for the response is also calculated. The two lines corresponding to the above two distributions are also shown in Fig. 5.30(c). If the three input variables are independent from one another, it is further possible to decompose the variance of the response into components which are contributed by each input variables. This indicates which input variable introduces the largest variability. The decomposition of the variance for the shortening is presented in Fig. 5.30(d).

The Bayesian prediction of long-time response by Latin hypercube sampling has been extended to segmentally constructed PC box girder bridges by Bažant and Kim (1987). They applied for this purpose the method of layered beam finite elements and developed a computer program (based on the Maxwell chain model) which can compare deflections measured during construction with the deflections predicted for the construction period, in order to update long-time sampling predictions. Figure (5.31) shows an example. The solid points represent the measured deflections used for updating while the empty points are the measured deflections which were for certain reasons ignored. Also, shown are the prior and posterior lines of mean deflection $\pm$ standard deviation. Once this method is refined to eliminate contamination of the measured deflections by temperature and humidity effects, it should make it possible to update the vertical alignment of the bridge segments that remain to be placed during construction so as better to satisfy long-time deflection specifications.

5.6.7 Analysis of concrete box girders

The effect of shear lag on creep deformations and stress redistributions in concrete box girder bridges has been analyzed both deterministically and stochastically by Křístek and Bažant (1985). It is found that the shear lag is as important for creep as it is for elastic deformations. Also, the statistical variability of material creep parameters and environmental factors has a significant effect on the statistical scatter of the calculated maximum longitudinal stresses and a very large effect on the statistical scatter of the predicted deflections.

In summary, the following conclusions are obtained (cf. Fig. 5.32):

1. Shear lag in box girder bridges, especially those with a small span-to-width ratio, is as important for long-time creep as it is for short-time elastic behaviour. Compared to bending theory predictions, the shear lag effect significantly increases the maximum values of the changes caused by a change

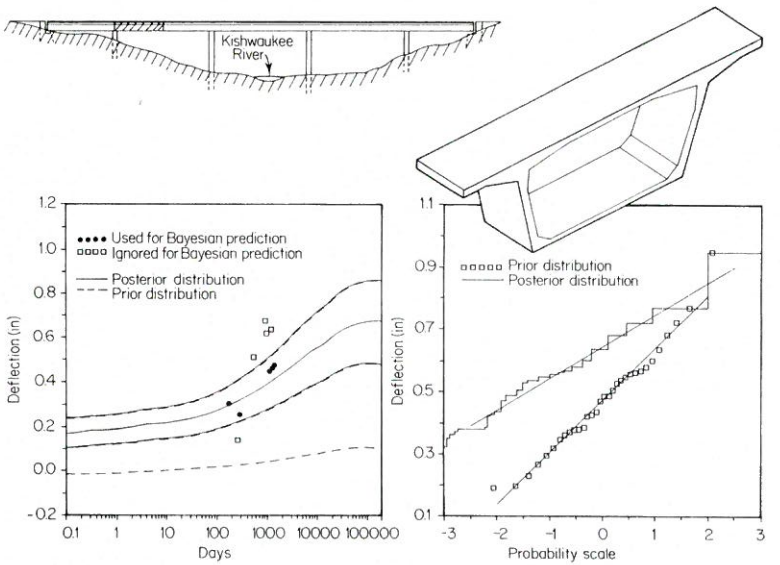

Figure 5.31 Prior and posterior deflection history predictions for a prestressed segmental box girder bridge (after Bažant and Kim, 1987)

of the structural system during construction, and causes a very large increase in the long-time deflection.

2. The statistical variability of material creep parameters and environmental factors is as important as the shear lag effect. It causes a significant statistical scatter in the predicted long-time stress values, and very large scatter in the predicted long-time deflections.
3. To achieve a reliable design of concrete box girder bridges from the viewpoint of long-time serviceability, both the shear lag effect and the statistical scatter must be taken into account in design.

5.6.8 Remarks

In summary, for simple beam-like structures (cf. Chapter 3), it is possible to use a quasi-elastic solution (e.g. Manuel and MacGregor, 1967; Bažant *et al.*, 1975; Bridge, 1979; Chiorino and Mola, 1982; Dilger, 1982a, b; Haas, 1982; Koprna, 1982; Lazić and Lazić, 1982; Bažant and Ong, 1983) to deal with random environmental changes. However, for general concrete structures subjected to random environmental changes, it is desirable to formulate the problem by a numerical method such as the FEM and the BEM, as used with deterministic

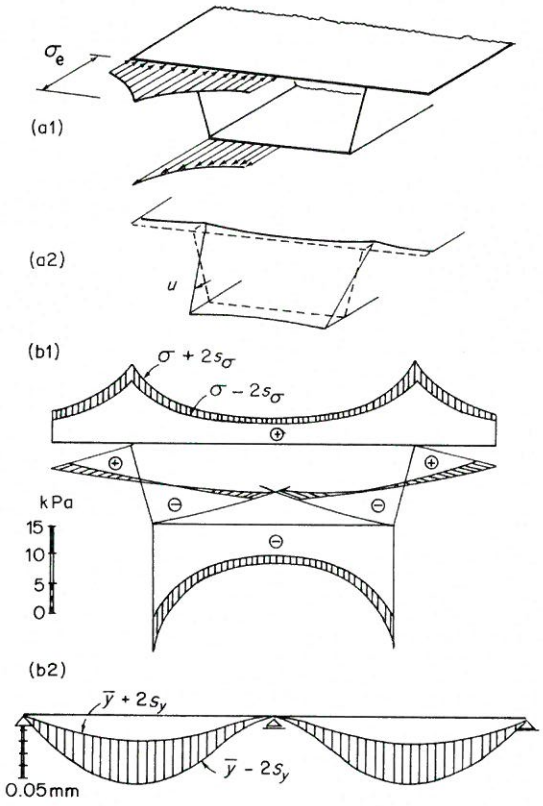

Figure 5.32 Shear lag effect on concrete box cross-section: (a) typical box cross-section and non-uniformity of longitudinal stress distribution caused by shear Lag (a1), and out-of-plane Warping (a2); (b) statistical results—95 per cent confidence limits for longitudinal stresses at support cross-section (b1), and for deflections at midspan (b2) (Křístek and Bažant, 1985) (1 kPa = 1.45×10^{-4} psi, 1 mm = 0.0394 in). Reproduced by permission of ASCE

creep models (cf. Chapter 9). For a stationary problem, it is possible to use the conventional FEM for creep analysis (Pister *et al.*, 1976; Argyris *et al.*, 1977; Smith and Anderson, 1978; Willam, 1978; Anderson, 1980; Bažant *et al.*, 1981a, b; Anderson, 1982). For ways of dealing with creep and relaxation data for numerical methods, see Bažant (1972a, 1982c) and Křístek and Šmerda (1982). The stochastic finite element scheme for structures with randomly distributed

material properties (e.g. Vanmarcke, 1983; Vanmarcke and Grigoriu, 1983; Tsubaki, 1986) will also be useful to obtain the statistics parameters.

5.7 SUMMARY AND CONCLUSIONS

In the first part of this chapter (Sections 5.2 and 5.3), the effect of stochastic material properties on creep is discussed. Some stochastic creep models based on the internal micromechanism of creep are introduced. They are used to extrapolate short-time creep data to obtain long-time creep prediction. In the second part (Section 5.4), the effect of other factors influencing the long-time creep prediction is discussed. Recent development in Bayesian prediction of creep and shrinkage parameters of a given concrete and Bayesian extrapolation of short-time creep and shrinkage data is also introduced. In the third part (Sections 5.5 and 5.6), the methods of analysing the effect of stochastic material properties and stochastic changes of environmental conditions and loads on concrete structures are discussed.

Some possible extensions regarding to the stochastic models for basic creep of concrete discussed in Section 5.3 may be listed as follows. Some of them have already been done to some extent, as given below.

1. Superposition of stresses at different times, which enables the model to deal with a general varying stress history such as unloading causing creep recovery. In order to deal with unloading, the mechanism of creep must be reconsidered. In the creep recovery phenomenon, the process is not increasing. Since a stochastic creep model is based on the micromechanism of creep, it is necessary to have a reasonable physical interpretation of the mechanism of creep recovery to deal with unloading in a general stress history.
2. Age dependence of the parameters involved in the model.
3. Non-linearity of creep such as low-stress non-linearity (adaptation) and high-stress non-linearity (flow), i.e. dependence on load duration and stress magnitude respectively. To make the model realistic and tractable, infinite divisibility of distribution of creep, as used in Benjamin *et al.* (1965) and Cinlar (1982) is essential. In the presence of non-linearity in stress, however, the additivity of deformation still holds, but the additivity of stress does not seem to hold. The effects of non-linearity of creep have been modelled for deterministic creep models in various manners. For example, see Bažant and Asghari (1977), Bažant and Kim (1979), Bažant and Tsubaki (1980a), and other references (Alda and Rostasy, 1980; Bažant and Tsubaki, 1980b; Creus, 1982; Bažant *et al.*, 1983). Experimental works on the non-linearity are also given in Freudenthal and Roll (1958), Harboe *et al.* (1958), Roll (1964), and Mamillan and Savin (1981).
4. Multidimensional stress history. See Ditlevsen (1982b).

To consider the micromechanism of creep and shrinkage of concrete of various

types, useful information may be obtained from the following experimental works on multiaxial creep (York *et al.*, 1970; Meyer, 1971; Ohgishi and Wada, 1973; McDonald, 1975), creep of high-strength concrete (Takahashi and Kawaguchi, 1980; Ngab *et al.*, 1982a, b; Bažant and Panula, 1984), creep of fly-ash concrete (Ghosh and Timusk, 1984), creep of lightweight-aggregate concrete (Arnaouti and Sangakkara, 1984), creep under cyclically varying dynamic loads (Suter and Mickelborough, 1975), effect of temperature on creep (Browne and Blundell, 1969; Kawasumi *et al.*, 1981; Nasser and Marzouk, 1981), effect of variable humidity (Bažant and Chern, 1985), effect of rate of drying (Day *et al.*, 1984), effect of age on relaxation (Trost, 1982), effect of sustained load on material constants (Hanson, 1953; Ross, 1958), and creep in tension (Pomeroy, 1982). For the effects of shrinkage and drying on concrete, see Wittmann (1968), Bažant and Najjar (1972), Jonasson (1978), Wittmann and Roelfstra (1980), Bažant and Raftshol (1982), Jonasson (1982), and Pihlajavaara (1982). The experimental works on this subject are, for example, Hanson (1968), Paul *et al.* (1981), Acker (1982), and Sakata (1983).

In addition to the methods described so far, there is another possibility to take into account—the effect of inhomogeneity of concrete on creep. For example, concrete may be treated as a heterogeneous composite material. Huet (1980, 1982a) reported a method of statistical treatment applied to a body made of a heterogeneous material to yield universal balance equations in local forms. This is an assimilation of the material to an effective continuum and leads statistical constitutive equations which needs experimental determination. Another review on this kind of treatment is shown by Dougill (1982). See also Counto (1966), Hobbs (1970), Kröner (1972), Shinozuka (1972), Kameswara Rao *et al.* (1974), Zaitsev and Wittmann (1974), and Shinozuka and Lenoe (1976).

On the methods of analysis to take into account the effect of the statistical variation of environmental conditions on concrete structures with creep and shrinkage, it has been reported that both the FEM and the BEM are effective. The latter is particularly efficient if the system is linear.

Also, the application of the probabilistic models in the reliability analysis of concrete structures should be considered, because it is the principal objective of constructing probabilistic models. However, it is not included in the scope of this chapter because its main purpose is to introduce probabilistic models used in uncertain analysis to obtain the variance as well as the mean value. In Madsen (1986), the application of the uncertain models in a reliability analysis is shown. This needs numerical methods to compute probabilities and provide sensitivity factors as a by-product (Madsen *et al.*, 1986). In addition, for the purpose of investigating the relative importance of various uncertainties involved in the creep and shrinkage of concrete, or assessing the parameter perturbation effects, sensitivity analysis (see, e.g. Frangopol, 1986) may be used.

Finally, it has become clear that considerable development has taken place in recent years in the area of probabilistic and statistical treatment of creep and shrinkage of concrete. Several mathematical models for creep and shrinkage of concrete that take into account their statistical variations and provide not only the mean value but also the upper and lower confidence limits of a certain specified probability cut-off are now available. Also, it seems that the experimental data to support these models have been accumulated. It is desirable to refine these models and to make them available for actual design purposes.

REFERENCES

ACI Committee 209/II (Chaired by D. E. Branson) (1971), Prediction of creep, shrinkage and temperature effects in concrete structures, ACI SP-27, *Designing for Effects of Creep, Shrinkage and Temperature*, American Concrete Institute, Detroit, Mich., pp. 51–93.

ACI Committee 435 (Chaired by B. L. Meyers) (1972), Variability of deflection of simply supported reinforced concrete beams, *American Concrete Institute Journal*, **69**(1), 29–35.

ACI Committee 209 (Chaired by J. A. Rhodes) (1982), Prediction of creep, shrinkage, and temperature effects in concrete structures, *ACI SP-76, Designing for Creep and Shrinkage in Concrete Structures*, American Concrete Institute, Detroit, Mich., pp. 193–301.

Acker, P. (1982), Drying of concrete: consequences for the evaluation of creep tests. In F. H. Wittmann (ed.), *Fundamental Research on Creep and Shrinkage of Concrete*, Martinus Nijhoff, The Hague, pp. 149–69.

Alda, W., and Rostasy, F. S. (1980), Zum Kriechen von Beton unter veraenderlicher einaxialer Druckbeanspruchung, Teil 2, *Betonwerk Fertigteil-Tech.*, **46**(7), 436–41.

Alou, F., and Wittman, F. H. (1982), Experimental study of the variability of shrinkage in concrete. In F. H. Wittmann (ed.), *Fundamental Research on Creep and Shrinkage of Concrete*, Martinus Nijhoff, The Hague, pp. 75–92.

American Concrete Institute (1983), *Building Code Requirements for Reinforced Concrete, ACI318-83*, Detroit, Michigan.

Anderson, C. A. (1980), *Numerical Creep Analysis of Structures*, Los Alamos Scientific Laboratory Report LA-UR-80-2585.

Anderson, C. A. (1982), Numerical creep Analysis of Structures. In Z. P. Bažant and F. H. Wittmann (eds), *Creep and Shrinkage in Concrete Structures*, Chap. 8, Wiley, New York, pp. 259–303.

Anderson, C. A., Whiteman, D. E., Smith, P. D., and Yao, J. T. P. (1978), A method for reliability analysis of concrete reactor vessels, Paper 78-PUP-100, presented at the Joint ASME/CSME Pressure Vessels and Piping Conference, Montreal, Canada.

Ang, A. H.-S., and Tang, W. H. (1975), *Probability Concepts in Engineering Planning and Design*, Wiley, New York, pp. 329–59.

Argyris, J. H., Pister, K. S., Szimmat, J., and Willam, K. J. (1977), Unified concepts of constitutive modeling and numerical solution methods for concrete creep problems, *Computer Methods in Applied Mechanics and Engineering*, **10**(2), 199–246.

Arnaouti, C., and Sangakkara, S. R. (1984), Creep and shrinkage in a lightweight-aggregate concrete, *Magazine of Concrete Research*, **36**(128), Sept., 165–73.

Bažant, Z. P. (1972a), Numerical determination of long-range stress history from strain history in concrete, *Materials and Structures*, **5**(27), 135–41.

Bažant, Z. P. (1972b), Thermodynamics of interacting continua with surfaces and creep analysis of concrete structures, *Nuclear Engineering and Design*, **20**(2), 477–505.

Bažant, Z. P. (1974), Theory of creep and shrinkage in concrete structures: a precis of recent developments, *Mechanics Today*, Vol. 2, Pergamon Press, New York, NY, pp. 1–93.